Applied Geochemistry 28 (2013) 220–234

Contents lists available at SciVerse ScienceDirect

Applied Geochemistry

journal homepage: www.elsevier.com/locate/apgeochem

Lead isotopic analysis within a multiproxy approach to trace pottery sources. The example of White Slip II sherds from Late Bronze Age sites in Cyprus and Syria

V. Renson [a,*], A. Martínez-Cortizas [b], N. Mattielli [c], J. Coenaerts [d], C. Sauvage [e], F. De Vleeschouwer [f], C. Lorre [g], F. Vanhaecke [h], R. Bindler [i], M. Rautman [j], K. Nys [d], Ph. Claeys [a]

[a] Earth System Science, Geology Department, Vrije Universiteit Brussel, Pleinlaan 2, 1050 Brussels, Belgium
[b] Departamento de Edafoloxía e Química Agrícola, University Santiago de Compostela, Fac. de Bioloxía, Campus Universitario Sur 15782 Santiago de Compostela (La Coruña), Spain
[c] Département des Sciences de la Terre et de l'Environnement, Université Libre de Bruxelles, Avenue F.D. Roosevelt 50, 1050 Brussels, Belgium
[d] Mediterranean Archaeological Research Institute, Vrije Universiteit Brussel, Pleinlaan 2, 1050 Brussels, Belgium
[e] Claremont Mckenna College, 500 E 9th Street, Claremont, CA 91711, USA
[f] EcoLab, Campus Ensat, Avenue de l'Agrobiopole,BP 32607, Auzeville Tolosane, 31326 Castanet-Tolosan, France
[g] Musée d'Archéologie Nationale, Château – Place C. de Gaulle, 78105 Saint-Germain-en-Laye, France
[h] Department of Analytical Chemistry, Ghent University, Krijgslaan 281-S12, 9000 Ghent, Belgium
[i] Department of Ecology and Environmental Science, Umeå University, SE-901 87 Umeå, Sweden
[j] Department of Art History and Archaeology, 109 Pickard Hall Columbia, MO 65211-1420, USA

ARTICLE INFO

Article history:
Received 3 April 2012
Accepted 7 October 2012
Available online 5 November 2012
Editorial handling by R. Fuge

ABSTRACT

Lead isotope analyses were carried out on fragments of White Slip II ware, a Late Bronze Age Cypriote pottery ware, and on raw materials possibly used for their production. Sherds originate from three Late Bronze Age sites (Hala Sultan Tekke and Sanidha in Cyprus and Minet el-Beida in Syria) and clays come from the surroundings of Sanidha, a production site for White Slip ware. X-ray fluorescence (XRF) and a Principal Component Analysis (PCA) are combined with Pb isotope analyses to further investigate the effectiveness of the latter method within a multiproxy approach for pottery provenance study. The pottery sherds from the three sites are compared between themselves and with potential raw material. Additional X-ray diffraction (XRD) and analyses using a scanning electron microscope (SEM) equipped with an energy dispersive X-ray detection (EDX) facility were performed on selected sherds and clays. This work confirms that the clay source used for pottery production in Sanidha derives from local weathered gabbro. It also shows that different origins can be proposed for White Slip II ware sherds from Hala Sultan Tekke and Minet el-Beida and that clays were prepared prior to White Slip II ware production. It finally confirms the effectiveness of Pb isotopes in tracing pottery provenance not only by comparing sherd assemblages but also by comparing sherds to potential raw materials.

1. Introduction

Pottery fragments constitute artifacts widely found at archaeological sites all around the world and their study documents numerous technological, economic and socio-cultural aspects of ancient civilizations. Among the questions commonly raised, that of their provenance often requires the use of a multiproxy approach. Elemental analyses are indeed widely and successfully applied to trace pottery origins (e.g., Knapp and Cherry, 1994; Gomez et al., 2002; Mommsen, 2003; Kennett et al., 2004; Asaro and Adan-Bayewitz, 2007; Ben-Shlomo et al., 2007; Tschegg et al., 2008, 2009). A recent study (Renson et al., 2011) established that Pb isotope analysis, so far rarely considered for this purpose, constitutes an efficient tool to identify pottery sources.

The main goal of the present study is to further investigate the effectiveness of isotopic analysis of Pb in pottery provenance studies using a multiproxy approach that not only compares pottery sets but also pottery and its potential raw materials. The latter remains an under-investigated field although successful examples exist (e.g. Adan-Bayewitz and Perlman, 1985; Tschegg et al., 2009).

White Slip ware, a hand-made pottery, characterized by a white or light slip applied on a dark clay and which most commonly has a hemispherical bowl shape (Popham, 1972), originates from Cyprus and was largely spread in the Eastern Mediterranean during the 14th and 13th centuries BC (Popham, 1972). The chemical and mineralogical composition (clay matrix, inclusions and slip) has been documented on fragments from several sites using different methods (Courtois and Velde, 1980; Artzy et al., 1981; Rautman et al., 1993; Gomez et al., 1995) and several authors have investigated the possible provenances of the different constitutive parts of the pottery (e.g., Gomez et al., 1995; Gomez and Doherty,

* Corresponding author. Tel.: +32 2 629 33 97.
E-mail address: vrenson@vub.ac.be (V. Renson).

0883-2927/$ - see front matter © 2012 Elsevier Ltd. All rights reserved.
http://dx.doi.org/10.1016/j.apgeochem.2012.10.025

2000). Although the entire foothills of the Troodos Mountains (corresponding to the Troodos Ophiolite located in central Cyprus, Fig. 1a) have been proposed as the source of the basaltic clay used for White Slip II production, Sanidha-*Moutti tou Ayiou Serkou* (hereafter Sanidha) is the only site, so far, where archaeological evidence attests to the existence of such production (Todd, 2000). Moreover, it was shown that the clay used for White Slip II ware production in Sanidha corresponded to smectite group clays resulting from the weathering of the leucocratic gabbros surrounding the site (Rautman et al., 1993; Gomez et al., 1995). Additionally, in Sanidha, aside White Slip, numerous Monochrome ware sherds were found which were also produced on the site. Monochrome ware represents an ordinary utilitarian pottery without painting or painted in a single color (Yon, 1981; Todd and Hadjicosti, 1991). In Sanidha, Monochrome ware presents no slip and occurs in a finer or coarser version respectively called Monochrome and Coarse Monochrome (Todd and Hadjicosti, 1991).

In the present study, the Pb isotopic variability, previously observed (Renson et al., 2011) within a set of 30 White Slip II sherds excavated in Hala Sultan Tekke, is compared to White Slip II sherds from Sanidha and to a larger set of clay sources collected in the surroundings of this site. In parallel, White Slip II sherds found in Minet el-Beida, the harbor of Ugarit (Syria), were also analyzed to explore their possible sources. More specifically, the aims of this study are to: (1) investigate the Pb isotopic composition of pottery sherds from the only attested White Slip II production center, namely Sanidha; (2) examine the compatibility of the isotopic composition of the White Slip II sherds from Hala Sultan Tekke previously analyzed (Renson et al., 2011) with that of Sanidha; (3) compare the Pb isotopic composition of White Slip II sherds with that of a set of clays (including clays derived from the weathering of gabbros from Sanidha area) and with the results of Gomez et al. (1995); (4) test the hypothesis that proposed clays from the Moni formation (silt and bentonite clays embedding fragments from various lithologies from the Triassic to the Upper Cretaceous, Fig. 1c) as a potential raw material for White Slip II production (Renson et al., 2011); and (5) scrutinize the compatibility of the isotopic composition of a set of White Slip II sherds excavated in Minet el-Beida (Syria) with that of an assemblage of White Slip II sherds and clays from Cyprus. Elemental chemistry determined by X-ray fluorescence (XRF) and subsequent Principal Component Analysis (PCA) are combined with the Pb isotope ratio data on selected sherds and clays to explore the significance of the Pb isotope signatures. To complement this study, elemental analyses were carried out on 4 sherds using a scanning electron microscope (SEM) equipped with an energy dispersive X-ray detection (EDX) system and the bulk mineralogy as well as the clay mineralogy of the sediments was identified using X-ray diffraction (XRD).

2. Archaeological settings of the pottery samples

2.1. Hala Sultan Tekke

The Late Bronze Age settlement of Hala Sultan Tekke lies on the west shore of the Larnaca salt lake in southeastern Cyprus (Fig. 1a). The material culture indicates that the town flourished from the second half of the 14th century BC to the first half of the 12th century BC. Undoubtedly, Hala Sultan Tekke is one of the Cypriot urban polities that actively participated in the Eastern Mediterranean exchange network, in particular during this timespan (Åström, 1986). White Slip sherds investigated here are mainly from the settlement and include sherds from a sherd deposit (F6031) studied by Öbrink (1979). Three samples (HST 13, 16 and 17) are from Tomb 24, located in the vicinity of the settlement (Åström and Nys, 2007). The Pb isotopic composition of this set of White Slip II sherds from Hala Sultan Tekke was investigated in a former paper (Renson et al., 2011) and archaeological contexts are detailed in Öbrink (1979), Åström and Nys (2007) and Renson et al. (2007).

2.2. Sanidha

The Late Bronze Age site of Sanidha is located in the foothills of the Troodos Mountains (Fig. 1a). The excavations revealed exceptionally important quantities of White Slip II and Monochrome fragments. Archaeological remains showed that Sanidha was a large-scale production center for these pottery wares (Todd, 2000, 2004). The site was already occupied in the Middle Bronze Age, but only became a pottery production center in the Late Bronze Age (Todd, 1990) and White Slip II material is dated to the Late Cypriote II (Todd, 1990) that ranges from the last quarter of the 15th century BC to the end of the 13th century BC (Knapp and Cherry, 1994; Eriksson, 2007). The site was not a permanent settlement, but was mainly devoted to the manufacture of pottery (Todd and Hadjicosti, 1991) and was probably connected in some

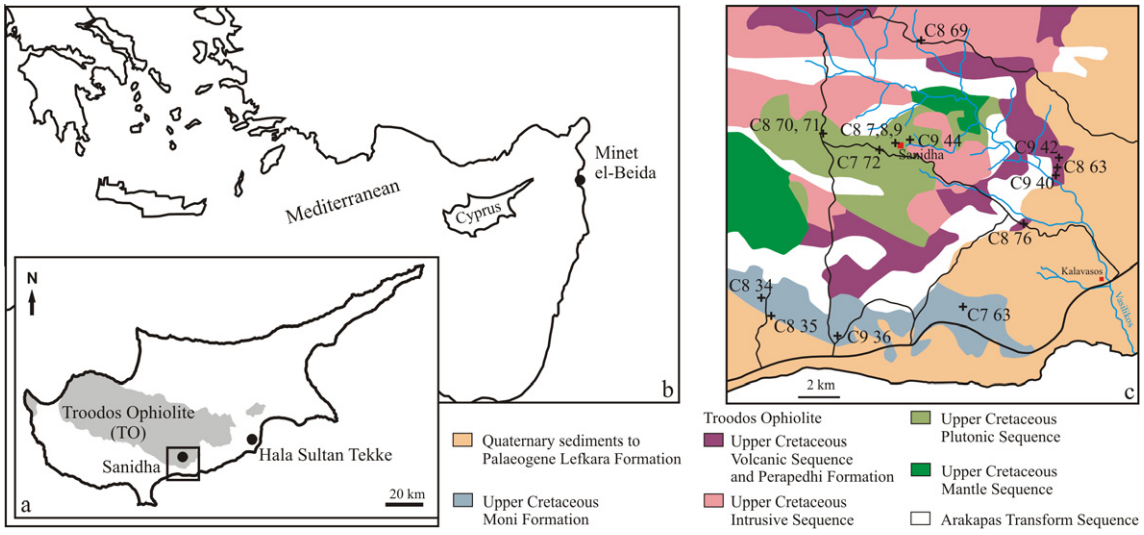

Fig. 1. (a and b) Location maps of the three sites studied here; (c) simplified geological map and location of the clay samples collected around Sanidha (samples C7 O 2 and C7 O 12 are not reported because they were collected at around 20 km from this area). Modified after the Geological Map of Cyprus (GSD, 1995).

way to the important contemporary site of Kalavasos-*Ayios Dhimitrios* located around 10 km SE (Todd, 2004). Petrographic analyses of White Slip II and Monochrome sherds from Sanidha indicated that the fabrics were similar and that the clay used for their production was identical (Xenophontos in Todd and Hadjicosti (1991)). Moreover, these authors suggested that the clays were probably local because the mineralogical composition of the sherds corresponded to that of raw material available around the site (Xenophontos in Todd and Hadjicosti (1991)). According to its chemical and mineralogical composition, White Slip II could originate from different locations of the circum-Troodos area, but so far Sanidha remains the only attested production center. A representative set of sherds was selected to define the Pb isotopic composition of Sanidha pottery production: 19 White Slip II sherds, 7 Monochrome sherds and 4 Coarse Monochrome sherds. All sherds came from the surface (Todd, 2004).

2.3. Minet el-Beida

Ugarit is situated on the Ras Shamra tell, on the northern Syrian coast (Fig. 1b) near modern Lattaquia. The site, capital of a kingdom of the same name, was occupied continuously from the end of the 8th until the end of the 2nd millennium BC, but is best known for its Late Bronze Age remains. It was ideally located at the junction of two major routes linking the coast and inner Syria and running along the Mediterranean. Because of this strategic position, its well-sheltered main harbor Minet el-Beida, and its natural resources, the site experienced great prosperity and was a major trade center, as demonstrated by imported materials (e.g., Schaeffer, 1949, pp. 136–233; Yon et al., 2000), and by international diplomatic correspondence and treaties written in Akkadian (Moran, 1992; Beckman, 1996; Lackenbacher, 2002). The 5 White Slip II and 6 White Slip II late sherds studied in this article come from the ashlar-built chamber tomb III [1005] located at Minet el-Beida (for the description of the tomb, its architecture, and a brief description of its material, see Schaeffer, 1929, p. 291; Schaeffer, 1949, pp. 144–149; Marchegay, 1999). White Slip II late corresponds to the final version of White Slip II and to a general deterioration of the ware with the use of coarser material, badly formed bowls, unevenly applied slip and more simplified painted decoration (Popham, 1972; Eriksson, 2007). In the chamber, the material found on the pavement included locally made oil lamps, Cypriot vases (White Slip II ware bowls, Monochrome ware bowls, and Base-ring ware bowls and juglets), Mycenaean ceramics, faience stirrup jars, Egyptian alabasters, metals, a cylinder seal, ivories, and the remains of three individuals. This tomb was probably used over a large period of time starting in the 14th c. BC until late in the 13th c. BC.

3. Clay samples

Sanidha is located in the Southern Troodos Transform Fault Zone, a geologically complex area, intensively faulted and characterized by rocks from the different sequences of the Troodos Ophiolite (Volcanic, Intrusive, Plutonic and Mantle sequences) and from the Transform sequence. In the SW and SE of this area, clays from the Upper Cretaceous Perapedhi, Kannaviou and Moni formations are developed (Fig. 1c). A set of 29 clays/soils was collected in the surroundings of Sanidha (less than 10 km, except samples C7 O 2 and O 12, located at 20 km). More precisely, samples were collected in the clays from the Moni formation (6), in the shales, umbers and clay from the Perapedhi formation (4), in clays derived from the weathering of the rocks from the Volcanic Sequence (3), the Intrusive Sequence (1) and the Plutonic Sequence (7, all weathered gabbros). Finally, samples of four soils were collected in the surroundings of Sanidha. The sampling in this area was carried out based on the geological maps published by the Geological Survey of Cyprus (Gass et al., 1994; GSD, 1995). Sediments were collected after the outcrop had been carefully cleaned and the coordinates of every sample were obtained using a GPS (Fig. 1c and Table 5). The set of clays analyzed here also includes samples previously measured for elemental composition by Rautman et al. (1993) and correspond to sediments from the Upper Cretaceous Kannaviou and Perapedhi formations and to a weathered gabbro sample. These latter samples are labeled as KKP.

4. Methods

4.1. Lead isotopic analysis

The samples were dried at 40 °C and milled in an agate mortar under an extracting hood. To remove any slip, painting or trace of weathering, the sherd surfaces were first entirely cleaned using a micro-drill equipped with diamond-bits, prior to crushing. The resulting powders were heated at 550 °C during 4 h. The acid digestions of the sample powders and subsequent Pb separation by ion exchange chromatography were carried out following the procedure described in Renson et al. (2011). Lead isotope ratios were measured using two multi-collector - inductively coupled plasma - mass spectrometers (MC-ICP-MS): a Nu Plasma (Nu Instruments) in operation at the Earth and Environmental Science Department of the "Université Libre de Bruxelles", Belgium, and a Thermo Scientific Neptune (Thermo Scientific) in operation at the Department of Analytical Chemistry of Ghent University, Belgium (the reproducibility of the measurements is discussed in Renson et al., 2011). The analytical conditions were identical to those described in Renson et al. (2011) and are only briefly summarized below. Thallium was added to each sample and to the standard to monitor and correct for instrumental mass discrimination. Sample solutions were prepared to obtain a beam intensity in the axial collector (^{204}Pb) of a minimum of 100 mV and a Pb/Tl ratio of $\sim$ 5, matching the Pb and Tl concentration ratio of the NIST SRM 981 "Common lead" isotopic standard (150 ng/g in Pb, with 50 ng/g in Tl). The NIST SRM 981 standard was measured several times before each analytical session and between each set of two samples on both devices (sample-standard bracketing). The standard values obtained agree with the long-term laboratory values and the MC-ICP-MS values of Weis et al. (2006). These values are also in agreement with thermal ionization mass spectrometry (TIMS) triple-spike values previously published by Galer and Abouchami (1998).

Some samples having lower Pb concentrations were analyzed using a DSN (Desolvating Nebuliser System) for sample introduction into the MC-ICP-MS unit. Thallium was also added to each sample and sample solutions were prepared to obtain a beam intensity in the axial collector (^{204}Pb) of a minimum of 100 mV and a Pb/Tl ratio of $\sim$ 4–5 corresponding to the Pb and Tl concentration ratio of the NIST SRM 981 "Common lead" isotopic standard (here 25 ng/g in Pb, with 6 ng/g in Tl). Values were corrected for instrumental mass discrimination using the NIST SRM 981 standard solution and the sample-standard bracketing method (White et al., 2000) and 5 replicates (i.e. second analysis of the same sample) and 5 duplicates (i.e. the entire procedure was reproduced on the same sample) were measured to test the reproducibility (Tables 4 and 5).

4.2. X-ray fluorescence

The concentrations of selected major and trace elements were measured on 300 mg of dried and homogenized powder using a Bruker S8 Tiger wavelength-dispersive X-ray Fluorescence

Table 1
(a) Bulk mineralogy of clay samples. UC for Upper Cretaceous. (b) Clay mineralogy of selected clay samples. UC for Upper Cretaceous.

Sample	Geological unit/formation	Quartz	Plagioclases	K-Feldspars	Calcite	Dolomite	Pyroxene	Amphibole	Clays	Cristobalite	Talc	Goethite	Muscovite	Serpentine
(a) Bulk mineralogy of clay samples. UC for Upper Cretaceous														
C7 63	Clay (UC Moni form.)	Present	Present						Major					
C8 34	Clay (UC Moni form.)	Present			Present				Abundant	Present				
C8 35a	Clay (UC Moni form.)	Present	Present						Major					
C8 35b	Clay (UC Moni form.)	Present			Present				Major					
C9 34	Clay (UC Moni form.)	Present							Major	Present				
C9 36	Clay (UC Moni form.)	Present							Major					
C8 63a	Umber (UC Perapedhi form.)	Present			Present				Present			Present		
C8 63b	Shale (UC Perapedhi form.)													
C8 76b	Shale (UC Perapedhi form.)	Present			Present				Abundant			Present		
C8 76a	Umber (UC Perapedhi form.)	Present							Major					
C7 O 12	Clay (UC Volcanic seq.)	Present	Abundant	Present		Trace			Abundant					Trace
C7 O 2 Alt	Clay (UC Volcanic seq.)	Trace							Abundant				Present	
C7 O 2 Rock	Rock (UC Volcanic seq.)	Present	Abundant				Present		Abundant					Trace
C8 11	Clay (UC Intrusive seq.)	Present							Abundant					
C8 71	Weathered gabbro	Trace	Abundant					Present	Abundant					
C8 8b	Weathered gabbro		Present				Present	Abundant	Abundant		Present			
C8 7	Weathered gabbro	Trace	Present				Present	Abundant	Present					
C8 8a	Weathered gabbro		Present					Abundant	Abundant		Present			Trace
C8 9b	Weathered gabbro	Present	Abundant				Present		Abundant					
C8 70	Weathered gabbro		Present					Present	Abundant					
C9 49	Weathered gabbro		Present					Abundant	Abundant		Present			
C7 72a	Weathered gabbro								Major					
C8 69a	Soil	Present	Present					Present	Abundant					
C9 40	Soil		Abundant	Present	Present		Present		Abundant					
C9 42	Soil		Abundant		Present				Abundant					
C9 44	Soil					Trace		Abundant	Abundant					

(b) Clay mineralogy of selected clay samples. UC for Upper Cretaceous

Sample	Geological unit/formation	Illite sheets in the Smectite-Illite Interstratified	
C7 63	Clay (UC Moni form.)	10–20%	
C8 34	Clay (UC Moni form.)	<10%	Illite?
C8 35a	Clay (UC Moni form.)	10–20%	Illite?
C9 34	Clay (UC Moni form.)	<10%	Illite
C9 36	Clay (UC Moni form.)	<10%	Illite?
C8 8b	Weathered gabbro	<10%	Illite, Degraded chlorite with vermiculite unstable interlayers
C9 44	Soil	<10%	Illite

(WD-XRF) analyzer in the Department of Ecology and Environmental Science at the University of Umeå, Sweden. Powders were transferred in 10 mm diameter plastic cups, with a 2.5 μm mylar film at the base. Each powder was slightly compressed manually to reduce porosity effects. A specific calibration was developed in order to optimize the WD-XRF approach for the matrices of the samples. The methodological details can be found in De Vleeschouwer et al. (2011). Briefly, it involved the development of a calibration procedure using certified reference materials that display the same matrices as the ceramic samples. Concentrations of the following elements were measured: Si, Ti, Al, Fe, Mn, Mg, Ca, Na, K, P, S, V, Ni, Cu, Zn, Rb, Sr and Pb.

4.3. Mineralogy of clay samples (XRD) and elemental analysis of selected sherds (SEM–EDX)

X-ray diffraction was used to describe the bulk mineralogy of the sediments (method description in Renson et al., 2011). Classification for quantitative estimations follows that proposed by Cook et al. (1975): trace, <5%; present, 5–25%; abundant, 25–65% and major, >65%. No correction factor is available for serpentine. However, because traces of this mineral were detected on a few spectra, it has been reported in Table 1a. The XRD methodology was also used to detail the clay mineralogy of selected sediment samples after elimination of the carbonates. Around 3 cm^3 of sample were gently dispersed in deionized water and sieved using a 63 μm mesh filter. Any carbonate was removed from the <63 μm fraction by adding dilute (0.1 M) HCl. The solution was then rinsed with deionized water to remove any trace of acid. The clay fraction (<2 μm) was separated by settling according to Stoke's law. Oriented mounts were prepared according to the procedure described in Moore and Reynolds (1989) and analyzed using a Brucker D8 Advance diffractometer. Each slide was analyzed three times: (1) after natural dry air conditions, (2) after ethylene–glycol solvation for 24 h, (3) after heating at 500 °C for 4 h. Clay species were identified using the resulting three diffraction spectra. The proportion of illite sheets in the interstratified smectite-illite was defined according to Moore and Reynolds (1989). Bulk mineralogy of samples KKP201, KKP202 and KKP204 was not determined.

Major elements of the sherd matrix were measured using a JEOL-JSM-6400 scanning electron microscope (SEM) equipped with an energy-dispersive X-ray detection (EDX) facility (Thermo Noran Pioneer with Si-Li detector) at 15 kV and a working distance of 39 mm. Carbon coating of the thin sections was carried out using an EMITECH-Carbon evaporation K450. Elemental mapping was conducted at several locations at various dimensions (460 μm × 580 μm or 1000 μm × 1500 μm) for each sherd. Several (8–14) measurements were then performed at various places on the matrix of each sherd. Minerals present as inclusions were also analyzed. The measurements were made on a single point representing the size of the beam (1 μm^2). No external standard was used.

4.4. Statistical analysis

A principal components analysis (PCA) was performed using the concentrations of Si, Ti, Al, Fe, Mn, Mg, Ca, Na, K, V, Ni, Cu, Zn, Rb, Sr, Pb and the $^{208}Pb/^{204}Pb$, $^{207}Pb/^{204}Pb$ and $^{206}Pb/^{204}Pb$ ratios. Phosphorus was not included in the analysis because it can be linked to post-depositional processes in a burial context (Freestone et al., 1985). As indicated by Baxter (1999), statistical analysis of compositional data is usually undertaken on transformed data. PCA was performed on two types of transformed data: (1) standardized concentrations (Z scores, $Z = (Xi - X_{avg})/SD$; where Xi is the value of an element in a given sample, X_{avg} is the average of all samples for that element and SD is the standard deviation), and (2) log (to base 10) transformation of concentrations. Transformations are applied to avoid the close data and scaling effects, and provide average centering.

Eight samples having largely different Pb isotopic or elemental composition were considered as gross outliers (in the sense applied by Baxter (1999)) and not included in the PCA because they strongly affected the results and limited the identification of the covariation structure. These were three clay samples (C7 63, C8 8a and C8 70) and five sherds (HST 4d, WS 33, WS 35, WS 36 and WS 70). After PCA analysis two clay samples (C9 42 and C9 44) were also found to be moderate outliers each one in a different principal component, but their elimination did not affect the extraction of the components or the distribution of the other samples (clays and sherds) on the projection of components (i.e. the ordination plots). Consequently, they were kept in the analysis.

The PCA was performed using a varimax rotation to maximize the variance of the elements in the principal components (Eriksson et al., 1999). A preliminary comparison produced almost identical results using the standardized and logged data, in agreement with what was found by Baxter (1995), which may be due to the elimination of the gross outliers (Baxter, 2001). Here, only the results obtained in the standardized data matrix are presented.

5. Results

5.1. Bulk and clay mineralogy of the sediments

The semi-quantitative results of the bulk mineralogy are reported in Table 1a. In the samples from the Moni formation, the main components are clay minerals; quartz is present in every sample. Plagioclase, calcite and cristobalite are also present but irregularly distributed across the Moni clay samples. Umbers (Fe, Mn-rich clays) and shales from the Perapedhi formation have a variable mineralogy: sample C8 63a contains amorphous material and the clay minerals, quartz, calcite and goethite are present; sample C8 63b is dominantly amorphous and the only mineral identified is goethite; clay minerals (mainly palygorskite) are abundant in samples C8 76b along with the presence of quartz, calcite and goethite and in C8 76a where quartz is also present. Samples from the Upper Cretaceous Volcanic sequence are mainly composed of clay minerals and quartz occurs (in traces or present). In some samples of this group, plagioclase, K-feldspar, dolomite, pyroxene, muscovite and serpentine can be identified in various proportions. The sample derived from the weathering of the Upper Cretaceous Intrusive sequence mainly consists of chlorite, with the presence of quartz. Samples from the weathered gabbros (Upper Cretaceous Plutonic sequence) are mainly composed of clay minerals. Sample C7 72a is a pure chlorite. The other samples from this group are also made of plagioclase. Amphibole is observed in most cases and less frequently, quartz, pyroxene, talc and serpentine. In the soil samples, clay minerals are also the main component. The assemblage of minerals observed in the soils is quite variable and details are reported in Table 1a.

The clay mineralogy of seven samples is presented in Table 1b.

5.2. SEM–EDX

In the four White Slip II sherds from Sanidha, the elemental composition of the clay matrix shows relatively high contents in SiO_2 and Al_2O_3 that vary from 41 to 66.3 wt.% and 4.1 to 36.5 wt.%, respectively (Table 2). This alumino-silicate matrix displays large variations in FeO, MgO and CaO, which range from 0 to 29.7 wt.%, from 0 to 17.4 wt.% and from 0.5 to 15.8 wt.%, respectively (Table 2). The TiO_2, Na_2O and K_2O contents vary from 0 to 5.4 wt.%, from 0 to 3.6 wt.% and from 0 to 2.6 wt.%, respectively (Table 2). The minerals observed in the thin sections of these pot-

Table 2
Major element composition obtained from SEM-EDX analysis of White Slip II from Sanidha. Total Fe as FeO. Values in wt.%. Traces of P_2O_5, Cr_2O_3, NiO and As_2O_3 were detected in some samples and are reported where they are above detection limits (0.15 wt.% for elements above Na).

Sample	SiO_2	TiO_2	Al_2O_3	FeO	MnO	MgO	CaO	Na_2O	K_2O	P_2O_5	Cr_2O_3	NiO	As_2O_3
San 24	53.06	0.36	24.47	12.02	0.00	3.20	5.00	1.45	0.43	0.00	0.00	0.00	0.00
San 24	54.35	0.49	22.31	12.04	0.00	6.21	3.25	0.77	0.58	0.00	0.00	0.00	0.00
San 24	56.22	0.00	26.65	2.83	0.49	0.00	9.09	3.58	0.29	0.00	0.00	0.00	0.86
San 24	51.03	0.94	4.08	17.34	0.78	14.14	10.61	0.88	0.19	0.00	0.00	0.00	0.00
San 24	53.97	0.00	33.00	0.00	0.00	8.38	1.94	0.45	2.26	0.00	0.00	0.00	0.00
San 24	52.38	0.36	6.88	15.31	0.00	13.73	11.17	0.00	0.18	0.00	0.00	0.00	0.00
San 24	51.88	5.39	23.72	11.77	0.00	2.16	3.91	0.81	0.35	0.00	0.00	0.00	0.00
San 24	55.73	0.36	26.10	11.06	0.00	3.68	2.02	0.60	0.44	0.00	0.00	0.00	0.00
San 27	55.95	3.41	17.64	12.73	0.00	4.04	4.06	1.05	1.13	0.00	0.00	0.00	0.00
San 27	63.85	0.00	19.70	3.45	0.00	1.25	9.10	1.44	1.20	0.00	0.00	0.00	0.00
San 27	54.43	0.57	25.89	9.53	0.00	4.88	1.99	0.66	2.04	0.00	0.00	0.00	0.00
San 27	54.72	0.00	6.08	18.85	0.00	17.43	2.55	0.00	0.37	0.00	0.00	0.00	0.00
San 27	57.65	0.00	24.73	7.84	0.00	4.37	4.56	0.86	0.00	0.00	0.00	0.00	0.00
San 27	54.73	0.00	26.08	9.70	0.00	5.12	1.91	0.79	1.67	0.00	0.00	0.00	0.00
San 27	56.19	0.41	18.30	12.11	0.00	8.90	2.03	0.60	1.46	0.00	0.00	0.00	0.00
San 27	40.96	0.43	26.67	14.12	0.00	5.55	12.27	0.00	0.00	0.00	0.00	0.00	0.00
San 27	60.15	0.29	21.11	7.11	0.00	5.53	4.45	0.78	0.58	0.00	0.00	0.00	0.00
San 27	50.96	0.00	15.96	11.58	0.00	11.35	9.47	0.67	0.00	0.00	0.00	0.00	0.00
San 27	56.70	0.00	10.84	13.66	0.00	13.35	3.98	0.84	0.64	0.00	0.00	0.00	0.00
San 27	65.69	0.00	20.72	2.38	0.00	0.00	6.27	2.52	1.12	0.00	0.00	0.00	1.28
San 27	53.48	0.42	7.07	17.14	0.00	15.48	5.81	0.28	0.00	0.00	0.00	0.32	0.00
San 27	48.86	1.66	11.48	13.68	0.00	15.28	7.94	0.00	0.00	0.00	1.11	0.00	0.00
San 28	52.83	1.26	11.58	29.73	0.57	0.95	1.59	0.73	0.77	0.00	0.00	0.00	0.00
San 28	59.74	0.00	24.60	5.32	0.00	2.76	5.73	1.34	0.51	0.00	0.00	0.00	0.00
San 28	66.03	0.00	20.30	5.17	0.00	2.57	4.35	1.41	0.16	0.00	0.00	0.00	0.00
San 28	48.72	0.00	30.66	2.44	0.00	1.20	15.84	0.88	0.26	0.00	0.00	0.00	0.00
San 28	61.41	0.00	21.65	5.29	0.00	1.61	6.16	2.25	1.63	0.00	0.00	0.00	0.00
San 28	63.52	0.00	20.76	7.15	0.00	3.34	3.99	1.03	0.21	0.00	0.00	0.00	0.00
San 28	58.53	0.61	8.62	16.57	0.00	10.50	4.32	0.85	0.00	0.00	0.00	0.00	0.00
San 28	57.03	0.00	25.19	9.88	0.00	4.99	1.60	0.78	0.24	0.29	0.00	0.00	0.00
San 28	48.56	0.45	26.30	14.90	0.00	4.89	3.72	0.98	0.19	0.00	0.00	0.00	0.00
San 28	66.29	0.00	22.42	5.63	0.00	2.47	1.80	1.03	0.36	0.00	0.00	0.00	0.00
San 28	51.95	0.50	28.59	8.83	0.00	4.32	3.49	1.66	0.66	0.00	0.00	0.00	0.00
San 28	54.91	0.00	36.54	3.05	0.00	0.76	1.62	1.89	1.23	0.00	0.00	0.00	0.00
San 28	55.92	0.00	25.55	9.71	0.00	4.25	3.07	1.07	0.43	0.00	0.00	0.00	0.00
San 30	62.80	0.00	20.84	10.51	0.00	3.76	1.50	0.59	0.00	0.00	0.00	0.00	0.00
San 30	60.71	0.54	20.10	14.17	0.00	2.58	1.27	0.43	0.21	0.00	0.00	0.00	0.00
San 30	46.84	0.43	24.76	22.78	0.00	3.08	1.51	0.00	0.60	0.00	0.00	0.00	0.00
San 30	57.71	0.54	21.95	11.22	0.00	2.92	1.87	1.15	2.63	0.00	0.00	0.00	0.00
San 30	54.11	0.00	25.91	8.83	0.00	4.63	2.59	2.16	1.78	0.00	0.00	0.00	0.00
San 30	54.42	0.59	24.90	12.00	0.00	4.07	1.04	1.42	1.55	0.00	0.00	0.00	0.00
San 30	48.20	0.53	26.28	17.43	0.00	3.49	1.51	0.51	2.05	0.00	0.00	0.00	0.00
San 30	60.41	0.00	17.77	7.48	0.00	5.81	6.54	1.15	0.84	0.00	0.00	0.00	0.00
San 30	50.34	0.00	5.08	24.85	0.00	13.73	5.61	0.39	0.00	0.00	0.00	0.00	0.00
San 30	56.27	1.40	22.80	14.02	0.00	4.63	0.55	0.33	0.00	0.00	0.00	0.00	0.00
San 30	57.74	0.00	4.52	19.76	0.00	16.21	0.61	0.48	0.69	0.00	0.00	0.00	0.00
San 30	53.46	0.91	22.61	13.07	0.00	3.59	5.70	0.65	0.00	0.00	0.00	0.00	0.00

tery fragments are pyroxene, plagioclase, magnetite, ilmenite, quartz, olivine, sphene and epidote. Similar data were obtained for six White Slip II sherds from Hala Sultan Tekke in Renson et al. (2011) and additional measurements were made on these sherds. Moreover, to present the chemical composition typical for the clay matrix, part of the data previously obtained and obviously corresponding to the composition of fresh minerals commonly present in the sherds was discarded. The values for SiO_2, Al_2O_3, FeO, MgO and CaO range from 41.5 to 69.7 wt.%, from 16.9 to 33.4 wt.%, from 0 to 11 wt.%, from 0.4 to 20.3 wt.% and from 0.6 to 18.3 wt.%, respectively. The TiO_2, Na_2O and K_2O contents vary from 0 to 2.1 wt.%, from 0 to 7.6 wt.% and from 0 to 6.8 wt.%, respectively. Minerals observed in thin sections, using SEM–EDX analysis, are pyroxene, plagioclases, magnetite, rutile, pseudorutile, ulvospinel, quartz, sphene, epidote, amphibole and chlorite.

5.3. XRF

The XRF results, as well as detection limits, accuracies and reproducibility are reported in Table 3. The concentrations of Si, Ti, Al, Fe, Mn, Mg, Ca, Na, K, P, S, V, Ni, Cu, Zn, Rb, Sr and Pb are displayed, as well as the average and standard deviation for each element in the different pottery and clay groups.

5.4. Lead isotope ratios

With the exception of the San 28 sample (with values of 15.704 and 18.977 for $^{207}Pb/^{204}Pb$ and $^{206}Pb/^{204}Pb$ ratios, respectively), all White Slip II sherds from Sanidha display a narrow range of values between 15.674 and 15.685 and between 18.853 and 18.976 for $^{207}Pb/^{204}Pb$ and $^{206}Pb/^{204}Pb$ ratios, respectively (Table 4 and Fig. 2a). The composition of the Coarse Monochrome varies from 15.677 to 15.686 and from 18.940 to 18.957 and that of the Monochrome from 15.671 to 15.684 and from 18.861 to 18.957 (Table 4 and Fig. 2a). The isotopic composition of the three wares from Sanidha is thus identical (Table 4 and Fig. 2a). The isotopic field of the White Slip II from Hala Sultan Tekke has a larger variability (Fig. 2b and c, see also Renson et al., 2011 for the values of the Pb isotope ratios). Except for two samples (WS 33 and WS 35) that show lower values in both ratios, the isotopic composition ranges from

Table 3
Elemental compositions measured by XRF. Results are given in % for major elements and in mg/g for trace elements. Values below detection limits are reported as <DL. Detection limits, standard deviation, accuracy and reproducibility are reported for each element.

Sample		Si %	Ti mg/g	Al %	Fe %	Mn mg/g	Mg %	Ca %	Na %	K %	P mg/g	S %	V mg/g	Ni mg/g	Cu mg/g	Zn mg/g	Rb mg/g	Sr mg/g	Pb mg/g
DL		0.028	0.015	0.012	0.007	0.005	0.01	0.005	0.007	0.002	0.2	0.002	0.004	0.002	0.003	0.003	0.002	0.003	0.004
STDEVA		1.56	0.00002	0.28	0.14	0.052	0.053	0.072	0.011	0.062	0.181	0.23	0.008	0.004	0.005	0.02	0.009	0.017	0.003
Acc. (%)		4	5	7	4	5	7	7	5	3	26	36	3	8	4	10	11	9	4
Repr. (%)		90	92	91	92	92	93	90	92	90	88	99	90	82	78	91	93	93	88
Clays																			
C7 63	UC Moni form.	27	6.3	3.2	4.5	0.79	1.6	1.7	0.79	1.72	0.9	0.08	0.154	0.092	0.052	0.10	0.062	0.19	0.022
C8 34	UC Moni form.	30	2.8	2.6	3	1.28	1.27	2.1	0.46	0.95	0.9	0.13	0.097	0.048	0.076	0.082	0.043	0.18	0.019
C8 35a	UC Moni form.	21.1	3.3	3.3	3.6	0.25	1.7	0.63	0.56	1.23	0.7	0.08	0.137	0.060	0.076	0.089	0.057	0.14	0.023
C8 35b	UC Moni form.	23.1	4.1	2.8	3.7	0.5	1.4	1.8	0.38	1.39	0.5	0.09	0.099	0.069	0.042	0.078	0.000	0.025	0.017
C9 34	UC Moni form.	22.7	3	2.6	2.7	1.13	1.33	0.66	0.54	0.82	0.6	0.1	0.103	0.039	0.048	0.067	0.030	0.078	<DL
C9 36	UC Moni form.	18.1	3	2.4	2.47	0.56	1.01	0.55	0.59	0.88	0.28	0.13	0.069	0.031	0.020	0.050	0.027	0.058	<DL
	Average	24	3.8	2.8	3.3	0.75	1.4	1.3	0.6	1.2	0.6	0.1	0.110	0.057	0.052	0.077	0.037	0.11	0.014
	Stand. Dev.	4.2	1.34	0.4	0.8	0.39	0.2	0.7	0.1	0.3	0.23	0.0	0.0310	0.022	0.021	0.017	0.023	0.068	0.010
C8 8a	Weather. gabbro	15.7	0.67	3.8	3.1	0.60	4.2	3.3	0.37	0.12	<DL	0.05	0.054	0.083	0.019	0.090	<DL	0.087	<DL
C8 8b	Weather. gabbro	20.9	1.84	3.8	4.4	0.84	5.6	4.4	0.5	0.18	0.25	0.06	0.134	0.21	0.024	0.054	<DL	0.066	<DL
C8 70	Weather. gabbro	21.7	1.43	4.7	4.2	0.84	6.1	5.5	0.85	0.03	0.29	0.05	0.100	0.091	0.019	0.053	0.062	0.12	0.011
KKP201	Weather. gabbro	20.2	3.9	5.5	6.0	0.53	2.1	2.1	0.72	0.33	0.38	0.07	0.236	0.059	0.139	0.052	0.011	0.083	0.006
C9 42	Soil	22	3.5	3.8	5.5	1.66	3.5	6.2	0.51	1.15	0.28	0.06	0.174	0.056	0.089	0.079	0.029	0.19	0.008
C9 44	Soil	25	1.16	1.5	6.7	1.44	9.4	6.2	0.12	0.06	0.25	0.06	0.121	0.61	0.000	0.060	0.015	0.023	0.010
	Average	21	2.1	3.9	5	0.98	5.2	4.6	0.51	0.31	0.27	0.06	0.137	0.18	0.048	0.065	0.020	0.095	0.006
	Stand. Dev.	3	1.31	1.3	1.3	0.46	2.5	1.7	0.26	0.42	0.07	0.01	0.063	0.22	0.054	0.016	0.023	0.056	0.004
Sherds																			
Hala Sultan Tekke																			
HST 4d	White Slip II	19.9	3.2	4.1	5.7	0.68	2.5	1.5	0.89	0.39	0.24	0.05	0.174	0.059	0.047	0.046	0.006	0.075	<DL
HST 13	White Slip IIA	20.5	3.9	4.9	6.2	0.78	2.6	2.5	0.49	0.3	0.5	0.06	0.251	0.055	0.098	0.048	0.004	0.19	0.009
HST 16	White Slip II	26	4	4.8	7.9	1.56	2.6	2.2	0.92	0.5	0.30	0.06	0.252	0.075	0.188	0.14	0.027	0.14	0.012
HST 17	White Slip II	20.5	3.2	3.7	5.7	1.28	2.4	1.5	0.69	0.61	0.5	0.05	0.167	0.044	0.141	0.13	0.013	0.12	<DL
HST 20	White Slip II late	10.3	1.34	2.1	2.2	0.22	1.19	1.04	0.35	0.14	<DL	0.05	0.064	0.013	0.007	0.021	0.003	0.12	<DL
WS 17	White Slip II	25	3.9	5.1	8	0.91	2.5	2.2	1.31	0.55	0.5	0.06	0.224	0.061	0.080	0.064	0.019	0.098	0.012
WS 27	White Slip II	22.4	3.2	4.6	6	0.83	2.6	2	1.31	0.38	0.33	0.06	0.191	0.054	0.031	0.050	0.012	0.081	0.004
WS 28	White Slip II	25	3.1	5.2	5.7	0.69	3.4	3.1	0.86	0.55	0.4	0.06	0.167	0.113	0.008	0.050	0.029	0.090	0.013
WS 33	White Slip II	19.3	2.1	4.3	4.5	0.60	3.2	2.1	0.63	0.35	0.27	0.06	0.128	0.097	0.003	0.039	0.010	0.062	0.005
WS 35	White Slip II	21.7	3.9	4	6.3	1.34	2.4	1.5	1.39	0.28	<DL	0.06	0.191	0.052	0.29	0.144	0.014	0.081	<DL
WS 36	White Slip II	19.9	2.3	4.6	4.8	0.63	3.3	2.3	0.67	0.37	0.20	0.06	0.141	0.108	<DL	0.042	0.013	0.065	0.005
WS 58	White Slip II	26	4.1	5.1	7.3	1.03	2.5	2.3	1.48	0.61	0.4	0.06	0.239	0.067	0.089	0.068	0.026	0.098	0.011
WS 59	White Slip II	23.5	4.1	4.9	7.6	0.97	2.5	2.2	1.21	0.55	0.28	0.06	0.223	0.069	0.065	0.063	0.021	0.097	0.009
WS 61	White Slip II	24.6	3.1	5.2	6	0.92	3.4	2.8	0.83	0.5	0.33	0.06	0.183	0.12	0.016	0.051	0.021	0.080	0.010
WS 65	White Slip II	20.5	3.4	4.5	7.7	0.68	2.3	1.7	0.81	0.44	0.29	0.05	0.181	0.059	0.027	0.050	0.016	0.076	0.007
WS 66	White Slip II	23.7	3.7	5	7.7	0.87	2.7	2.2	1.31	0.52	0.4	0.06	0.210	0.064	0.089	0.059	0.017	0.096	0.011
WS 69	White Slip II	22.3	2.9	5	5.3	0.59	3.1	2.3	0.85	0.81	0.33	0.05	0.195	0.067	0.011	0.042	0.008	0.094	0.005
WS 70	White Slip II	19.6	3.3	4	6.1	0.85	2.3	1.8	0.9	0.27	0.29	0.05	0.167	0.045	0.32	0.43	0.015	0.083	0.006
	Average	22	3.3	4.5	6.2	0.86	2.65	2.07	0.94	0.45	0.32	0.06	0.186	0.068	0.084	0.085	0.015	0.097	0.007
	Stand. Dev.	4	0.75	0.75	1.45	0.31	0.53	0.51	0.33	0.16	0.11	0.00	0.046	0.027	0.095	0.094	0.008	0.031	0.004
Sanidha																			
San 13	White Slip II late	24.3	3.6	5.1	6.8	1.28	3.3	2.8	0.56	0.54	0.29	0.06	0.232	0.15	0.030	0.047	0.014	0.094	0.006
San 14	White Slip II late	23.1	3.1	5.2	6	0.74	2.4	2.4	0.66	0.35	<DL	0.06	0.185	0.14	0.022	0.049	0.013	0.103	0.009
San 16	White Slip II	22.6	3.5	5.5	5.9	0.87	3.2	2.8	0.66	0.71	0.5	0.06	0.195	0.097	0.011	0.046	0.018	0.085	0.012
San 18	White Slip II	23	3.3	5.3	5.7	0.64	3	2.4	1.04	0.84	0.22	0.06	0.225	0.064	0.011	0.044	0.019	0.11	0.007
San 20	White Slip II	25	3.3	5.8	6.6	0.90	3.3	2.5	0.53	0.61	0.38	0.06	0.193	0.092	0.008	0.044	0.026	0.072	0.009
San 23	White Slip II	23.5	3.7	5.4	6.1	0.95	3.2	2.6	0.6	0.52	0.32	0.06	0.196	0.15	0.036	0.056	0.032	0.068	0.011
San 24	White Slip II	19.7	3.6	4.7	5.5	0.74	2.1	1.9	0.8	0.3	0.22	0.05	0.214	0.057	0.044	0.049	0.009	0.063	<DL

San 27	White Slip II	22.9	3.5	5.4	6.1	0.68	2.9	2.4	0.96	0.69	0.26	0.06	0.215	0.082	0.018	0.045	0.022	0.100	0.009
San 28	White Slip II	24.2	2.9	6.3	6.5	0.96	3	2.6	0.69	0.3	0.36	0.05	0.202	0.084	0.052	0.061	0.019	0.073	0.017
San 29	White Slip II	21.7	3.8	4.7	5.7	0.79	2.4	2	0.84	0.31	0.28	0.05	0.208	0.062	0.034	0.044	0.016	0.070	0.006
	Average	23	3.4	5.3	6.1	0.86	2.88	2.44	0.73	0.52	0.30	0.06	0.207	0.098	0.027	0.049	0.019	0.084	0.009
	Stand. Dev.	1	0.28	0.48	0.42	0.184	0.43	0.30	0.17	0.20	0.10	0.00	0.0150	0.036	0.015	0.006	0.007	0.016	0.004
Minet el-Beida																			
MeB 2	White Slip II	16.6	1.83	3.3	3.4	0.45	2.5	1.8	0.46	0.2	<DL	0.06	0.091	0.068	0.013	0.029	0.005	0.053	<DL
MeB 3	White Slip II	25	3.3	5.1	6.1	0.86	3.4	3.3	0.63	0.35	0.38	0.06	0.170	0.15	0.045	0.056	0.039	0.11	0.009
MeB 4	White Slip II	25	2.9	4.9	5.8	1.01	3.9	2.9	0.69	0.46	0.35	0.06	0.168	0.17	0.007	0.054	0.022	0.073	0.014
MeB 5	White Slip II	22.4	3	4.8	6	0.82	3	2.8	0.42	0.36	0.4	0.08	0.194	0.18	0.083	0.066	0.017	0.094	0.012
MeB 6	White Slip II	18.3	2.7	4.1	5.1	0.66	2.8	2.4	0.39	0.3	0.33	0.06	0.155	0.15	0.066	0.053	0.015	0.085	<DL
MeB 10	White Slip II late	23	3.6	4.8	5.8	0.78	2	3	0.55	0.24	0.6	0.06	0.198	0.112	0.101	0.081	0.019	0.14	0.017
MeB 16	White Slip II late	16.9	3	4.3	4.7	0.62	1.8	2.1	0.51	0.23	0.26	0.06	0.167	0.066	0.157	0.049	0.013	0.068	0.012
MeB 17	White Slip II late	23	3.3	5.4	5.8	0.75	2.7	3	0.83	0.28	<DL	0.06	0.188	0.074	0.077	0.063	0.012	0.086	0.008
	Average	21	3	4.6	5.3	0.74	2.76	2.67	0.56	0.30	0.33	0.06	0.166	0.12	0.069	0.056	0.018	0.089	0.01
	Stand. Dev.	4	0.54	0.66	0.92	0.171	0.69	0.52	0.15	0.08	0.15	0.01	0.034	0.045	0.049	0.015	0.010	0.027	0.006

15.666 to 15.684 and from 18.737 to 18.981 for $^{207}Pb/^{204}Pb$ and $^{206}Pb/^{204}Pb$ ratios, respectively. The majority of White Slip II samples from Hala Sultan Tekke (24 out of 31) plot in the range of the Sanidha production (Fig. 2b and c). White Slip II sherds from Minet el-Beida have values ranging from 15.681 to 15.697 and from 18.872 to 18.991 for $^{207}Pb/^{204}Pb$ and $^{206}Pb/^{204}Pb$ ratios (Table 4 and Fig. 2b). The White Slip sherds from Minet el-Beida can be divided into two groups according to their Pb isotopic composition. Three White Slip II sherds have a signature compatible with that of White Slip II from Sanidha, while the others (2 White Slip II and 6 White Slip II late) are spread along a trend that does not overlap with the main cluster (Fig. 2b).

The different clay samples analyzed show a large isotopic variability and few display a Pb isotopic composition that falls within the field of White Slip II sherds (Table 5 and Fig. 2c). Among them, the clays from the Moni formation have isotopic values that range between 15.666 and 15.689 and between 18.812 and 18.926 for $^{207}Pb/^{204}Pb$ and $^{206}Pb/^{204}Pb$, respectively. The isotopic values of the bentonitic clay from the Kannaviou formation are 15.662 and 18.812. Values for the umbers and shales from the Perapedhi formation range between 15.592 and 15.629 and between 18.516 and 18.724, while values for the bentonitic clay of this formation are 15.665 and 18.834. Clays and rock from the Upper Cretaceous Volcanic sequence display values that range from 15.601 to 15.612 and from 18.829 to 18.904. Values for the sample derived from the weathering of the Upper Cretaceous Intrusive sequence are 15.640 and 19.274. The weathering products of the gabbros (Upper Cretaceous Plutonic sequence) have values that range from 15.573 to 15.713 and from 18.526 to 21.531. The values for the soil samples are between 15.593 and 15.684 and between 18.846 and 18.878, for $^{207}Pb/^{204}Pb$ and $^{206}Pb/^{204}Pb$ ratios, respectively. Finally, for sample C7 72a, a pure chlorite, the $^{207}Pb/^{204}Pb$ and $^{206}Pb/^{204}Pb$ ratios are 15.957 and 25.275.

Only four clay samples have a composition that corresponds with the field of the Sanidha production (Table 5 and Fig. 2c): two clays from the Moni formation (C7 63 and C9 34) and two clays derived from the weathering of the gabbros (C8 8b and KKP201). Seven other clays have a Pb isotopic composition similar to that of the Sanidha production and these range between 15.662 and 15.689 and 18.812 and 18.859 for the $^{207}Pb/^{204}Pb$ and $^{206}Pb/^{204}Pb$ ratios, respectively. These clay samples are: four clays from the Moni formation (C8 34, C8 35a, C8 35b and C9 36), one from the Kannaviou formation (KKP204), one from the Perapedhi formation (KKP202) and one soil developed in Sanidha (C9 44).

6. Discussion

The Sanidha White Slip II sherds analyzed show an alumino-silicate matrix, the composition of which is compatible with that of a smectite. The composition of the "matrix" shows large variability in SiO_2, Al_2O_3, FeO, MgO and CaO that can be explained by the elemental replacements normally occurring in smectite clay. The composition of the matrix of the White Slip II sherds from Hala Sultan Tekke resembles that of White Slip II sherds from Sanidha, though Al_2O_3 and FeO contents show a greater range of variability. The assemblage of minerals present as inclusions is also similar in White Slip sherds from both Sanidha and Hala Sultan Tekke. The matrix composition and the mineral assemblage, as indicated by the SEM-EDX analyses, match the composition of the material resulting from the weathering of basaltic rocks (local gabbros). More specifically, the presence of a few minerals, such as quartz, chlorite and epidote, indicates that the gabbro is characterized by a greenschist facies and low-grade metamorphism. Courtois and Velde (1989) have already reported the greenschist facies mineralogy. These observations also agree well with the results

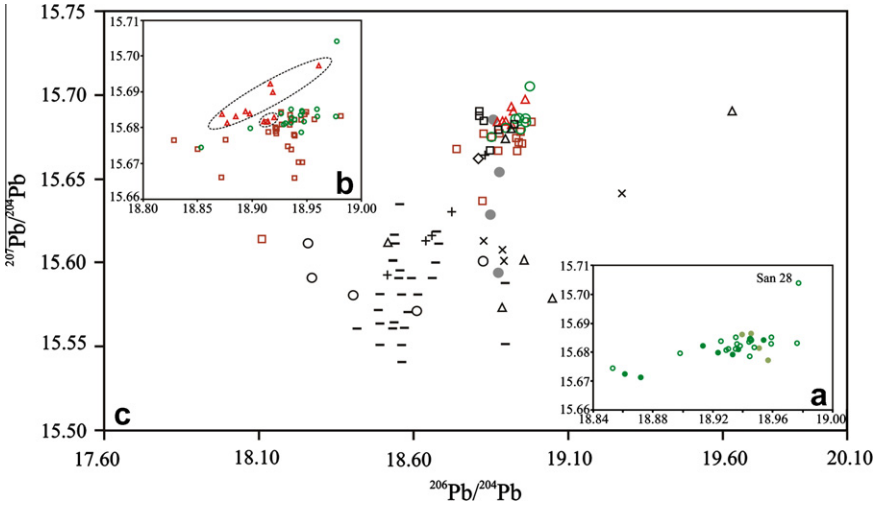

Fig. 2. (a) $^{207}Pb/^{204}Pb$ vs $^{206}Pb/^{204}Pb$ three-isotope plot for Sanidha sherds. Open circles, White Slip II; dark green circles, Monochrome and light green circles, Coarse Monochrome; (b) $^{207}Pb/^{204}Pb$ vs $^{206}Pb/^{204}Pb$ three-isotope plot for White Slip II sherds from the three sites. Detail between 15.66 and 15.71 and between 18.80 and 19.00 for $^{207}Pb/^{204}Pb$ and $^{206}Pb/^{204}Pb$, respectively. Green circles, White Slip II from Sanidha; brown squares, White Slip II from Hala Sultan Tekke and red triangles, White Slip II from Minet el-Beida. The two groups of White Slip II sherds from Minet el-Beida are surrounded by ellipses; (c) $^{207}Pb/^{204}Pb$ vs $^{206}Pb/^{204}Pb$ three-isotope plot for White Slip II sherds from the three sites, clays around Sanidha (this study), fresh gabbro (from Spooner and Gale (1982) and Hamelin et al. (1984)) and sulfides (from Spooner and Gale (1982), Hamelin et al. (1988) and Booij et al. (2000)). Green circles, White Slip II from Sanidha; brown squares, White Slip II from Hala Sultan Tekke; red triangles, White Slip II from Minet el-Beida; open squares, Moni formation; open diamond, Kannaviou formation; crosses, Perapedhi formation; Saint Andrews crosses, Upper Cretaceous Volcanic sequence and Intrusive sequence; open triangles, weathered gabbro; black circles, soils; open circles, fresh gabbro and dashes, sulfides. Samples C7 72a and C8 9b have very high $^{207}Pb/^{204}Pb$ and $^{206}Pb/^{204}Pb$ values and are not reported on the plot for clarity reasons. No leaching process was applied to clay samples measured in this study prior to analysis.

of petrographic analysis of Sanidha sherds made by Xenophontos (in Todd and Hadjicosti, 1991). To summarize the petrographic, XRF and XRD studies, the pottery fragments do have the typical mineralogical composition of White Slip II sherds previously analyzed and whose fabric was shown to be unique and most likely derived from the basic or ultrabasic material of the Troodos Ophiolite (Artzy et al., 1981).

The Pb isotopic composition of the 30 sherds representing three pottery wares from Sanidha (Monochrome, Coarse Monochrome and White Slip II) plots within a narrow field (Fig. 2a). This homogeneity supports the assumption that a single and fairly uniform clay source was used as base material for the production of White Slip II and Monochrome (including Coarse Monochrome) in Sanidha, in agreement with the petrographic data (Xenophontos in Todd and Hadjicosti, 1991). Most of the White Slip II sherds from Hala Sultan Tekke have a Pb isotopic composition similar to that of White Slip II from Sanidha (Fig. 2b and c). However, it is obvious that a few of them differ from the Pb isotope ratios typical for Sanidha sherds (Fig. 2c). Seven White Slip II sherds from Hala Sultan Tekke indeed extend along a trend between the main Sanidha cluster and lower $^{207}Pb/^{204}Pb$ values (Fig. 2b and c), while three others are isolated and display lower values in $^{207}Pb/^{204}Pb$ or in both $^{207}Pb/^{204}Pb$ and $^{206}Pb/^{204}Pb$ ratios (Fig. 2c). It is important to note that SEM-EDX analysis carried out on the clay matrix and on the mineral assemblage present as inclusions did not reveal any mineralogical differences between sherds that plot inside and outside the cluster. The presence of accessory minerals bearing exotic Pb isotopic ratios compared to those of the clay-matrix minerals can most likely be ruled out to explain this isotopic variability. In magmatic rocks, common Pb is in the plagioclases and K-feldspars while radiogenic Pb is found in the accessory minerals. In most cases, because of mass balance, the Pb isotopic composition of the whole rock is consequently more similar to that of the feldspars and plagioclases than to that of the accessory minerals (Harlavan et al., 1998). The isotopic composition of the White Slip II is thus most likely dominated by that of the clays derived from the weathering of the dominant minerals constituting the gabbros.

The $^{207}Pb/^{204}Pb$ vs $^{206}Pb/^{204}Pb$ three-isotope plot (Fig. 2c) shows that the isotopic composition of the White Slip II cluster is similar to that of different types of clay: the ones derived from the weathering of the gabbros, some clays from the Moni formation, and a soil collected in Sanidha. An interstratified smectite-illite rich in smectite sheets dominates the clay mineralogy of these samples. The different clays derived from the weathering of the gabbros were all collected in the vicinity of Sanidha (<5 km), but display highly variable Pb isotopic composition. Some of them have a signature compatible with that of fresh gabbros from the Troodos Ophiolite (Fig. 2c). One sample has very high values of both $^{207}Pb/^{204}Pb$ and $^{206}Pb/^{204}Pb$ ratios (15.690 and 19.629, respectively). The Pb isotopic composition of two samples (C8 8b and KKP201) is compatible with that of the White Slip II (Fig. 2c). The latter two weathered gabbro samples have values higher than those of the fresh rocks either for the $^{206}Pb/^{204}Pb$ ratio or for both the $^{207}Pb/^{204}Pb$ and the $^{206}Pb/^{204}Pb$ ratios. Nobre-Silva et al. (2009) observed a similar shift in the isotopic composition of Pb in basalts, linked to the weathering process. These authors indeed showed that the weathered basalts had higher values of both $^{207}Pb/^{204}Pb$ and $^{206}Pb/^{204}Pb$ ratios and a higher dispersion than the fresh basalt samples. This isotopic shift most likely accounts for the difference previously observed between the signature of White Slip II sherds and that of the fresh gabbros (Renson et al., 2011).

6.1. Principal component analysis

To discriminate between the different possible clay sources and to further explain the different isotopic composition in the White Slip II fragments investigated here, a PCA was performed on the Pb isotope ratios and the elemental concentrations for selected clay samples and White Slip II sherds. As indicated in the methods section, eight samples were considered as gross outliers and not included in the PCA (clay samples C7 63, C8 8a and C8 70 and sherds HST4d, WS 33, WS 35, WS 36 and WS 70).

Five principal components account for 80.4% of the variance of the chemical and isotopic composition (Fig. 3a). The first

Table 4
Lead isotope ratios of Sanidha and Minet el-Beida sherds. 2se refers to 2 standard errors (internal error).

Sample		$^{208}Pb/^{204}Pb$	2se	$^{207}Pb/^{204}Pb$	2se	$^{206}Pb/^{204}Pb$	2se
Sanidha							
San 1	Coarse Monochrome	39.0148	0.0030	15.6773	0.0011	18.9568	0.0013
San 2	Coarse Monochrome	39.0212	0.0017	15.6814	0.0006	18.9511	0.0007
San 3	Coarse Monochrome	39.0176	0.0020	15.6864	0.0007	18.9453	0.0008
San 4	Coarse Monochrome	39.0160	0.0023	15.6860	0.0008	18.9396	0.0008
San 5	Monochrome	39.0164	0.0022	15.6792	0.0008	18.9330	0.0008
San 6	Monochrome	39.0239	0.0020	15.6810	0.0007	18.9368	0.0007
San 7	Monochrome	39.0232	0.0020	15.6842	0.0006	18.9538	0.0006
San 8	Monochrome	39.0050	0.0025	15.6823	0.0008	18.9132	0.0008
San 9	Monochrome	38.9323	0.0024	15.6714	0.0008	18.8718	0.0009
San 10	Monochrome	39.0012	0.0023	15.6798	0.0008	18.9234	0.0008
San 11	Monochrome	38.9278	0.0019	15.6725	0.0006	18.8610	0.0006
San 12	White Slip II late	39.0301	0.0018	15.6850	0.0006	18.9354	0.0006
San 13	White Slip II late	39.0718	0.0025	15.6846	0.0009	18.9450	0.0009
San 14	White Slip II late	39.0252	0.0025	15.6813	0.0009	18.9351	0.0010
San 15	White Slip II	39.0149	0.0027	15.6786	0.0010	18.9444	0.0010
San 16	White Slip II	39.0393	0.0024	15.6821	0.0008	18.9381	0.0009
San 17	White Slip II	39.0362	0.0021	15.6835	0.0007	18.9440	0.0008
San 18	White Slip II	39.0298	0.0021	15.6831	0.0007	18.9761	0.0008
San 19	White Slip II	39.0336	0.0024	15.6808	0.0008	18.9288	0.0009
San 20	White Slip II	39.0673	0.0027	15.6827	0.0009	18.9359	0.0009
San 21	White Slip II	39.0553	0.0027	15.6843	0.0009	18.9455	0.0009
San 22	White Slip II	39.0449	0.0028	15.6839	0.0010	18.9257	0.0010
San 23	White Slip II	39.0180		15.6798		18.8981	
San 24	White Slip II	38.9579	0.0027	15.6743	0.0009	18.8529	0.0009
San 25	White Slip II	39.0490	0.0025	15.6816	0.0008	18.9473	0.0009
San 26	White Slip II	39.0733		15.6850		18.9588	
San 27	White Slip II	39.0338	0.0025	15.6830	0.0008	18.9591	0.0008
San 28	White Slip II	39.0395	0.0019	15.7039	0.0006	18.9772	0.0007
San 28*		39.0443	0.0030	15.7039	0.0011	18.9788	0.0011
San 29	White Slip II	39.0729	0.0028	15.6811	0.0010	18.9302	0.0009
San 30	White Slip II	39.0414	0.0024	15.6844	0.0008	18.9449	0.0008
Minet el-Beida							
MeB 2	White Slip II	38.9999	0.0024	15.6818	0.0008	18.9142	0.0010
MeB 3	White Slip II	39.0006	0.0026	15.6827	0.0009	18.9199	0.0009
MeB 4	White Slip II	39.0111	0.0024	15.6817	0.0009	18.9105	0.0010
MeB 5	White Slip II	38.9516	0.0019	15.6813	0.0008	18.8769	0.0010
MeB 5*		38.9508	0.0023	15.6809	0.0009	18.8758	0.0010
MeB 6	White Slip II	38.9589	0.0032	15.6830	0.0012	18.8845	0.0013
MeB 9	White Slip II late	38.9766	0.0023	15.6838	0.0008	18.8976	0.0008
MeB 9**		38.9768	0.0020	15.6843	0.0007	18.8979	0.0008
MeB 10	White Slip II late	38.9859	0.0024	15.6897	0.0009	18.9188	0.0013
MeB 11	White Slip II late	38.9746	0.0027	15.6844	0.0010	18.8936	0.0011
MeB 15	White Slip II late	38.9938	0.0032	15.6922	0.0012	18.9162	0.0013
MeB 16	White Slip II late	39.0331	0.0025	15.6972	0.0009	18.9607	0.0011
MeB 17	White Slip II late	38.9563	0.0021	15.6836	0.0007	18.8723	0.0009

* Duplicate.
** Replicate.

component, C1 (23% of total variance), is associated with large positive loadings of V, Fe, Al, Na and $^{206}Pb/^{204}Pb$ ratios (0.72–0.90) and a moderate positive loading of the $^{208}Pb/^{204}Pb$ ratio (0.62) and Ti (0.53) (Fig. 3a and b). The C1 scores mainly separate the clays (negative scores) from the pottery fragments (positive scores), excepted for sample KKP201, which has a positive score as for the sherds (Fig. 4a). Moreover, on the basis of the scores for C1 in the different pottery groups, it seems that White Slip sherds (White Slip II and White Slip II late) from Minet el-Beida differ from those of Sanidha and Hala Sultan Tekke, while the White Slip II sherds from Sanidha and Hala Sultan Tekke are clearly similar. Vanadium, Fe, Al and Ti are elements that tend to concentrate in the clay fraction of soils and weathering products. The positive scores in C1 observed in the pottery fragments thus indicate an enrichment in fine size grains in comparison with the clays of the area, which could be the result of an intentional man-made grain size selection. Such a selection can be confirmed by comparing the results of samples C8 8b to KKP201. Indeed, these two samples, collected close to each other (< 1 km), both correspond to weathering products of the gabbros from Sanidha and have a similar Pb isotopic composition, compatible with that of Sanidha White Slip II. However, different grain-size selection processes were applied to these samples. Indeed, on one hand no grain size selection was performed on sample C8 8b prior to analyses but on the other hand sample KKP201 was sieved to < 63 μm and only the fine grain size fraction was studied. The large similarity in C1 scores in KKP201 and White Slip II is evidence for a grain-size selection process applied to the raw material prior to pottery production (Fig. 4b).

The second component, C2 (20% of variance), is associated with large positive loadings of Mg, Ca and Ni (0.82–0.95) and a moderate negative loading of Ti (−0.60) (Fig. 3a and b). This component mainly accounts for differences in the clays (Fig. 4a and b) and separates the Moni samples (high negative scores) from the weathered gabbros and the soils (high positive scores). It does not distinguish either the pottery fragments, or sample KKP201, which show quite similar factor scores with values close to zero. The elements of C2 indicate a mafic mineralogy. The fact that sample KKP201 does not have a large score suggests that this variation in composition captured by C2 relates to minerals present in the coarser fraction of the clays.

Table 5
Lead isotope ratios and coordinates of clay samples. 2se refers to 2 standard errors (internal error). UC for Upper Cretaceous. Values in italics refer to data previously published in Renson et al. (2011).

Sample		Geological unit/formation	$^{208}Pb/^{204}Pb$	2se	$^{207}Pb/^{204}Pb$	2se	$^{206}Pb/^{204}Pb$	2se	Lat. N	Long. E
C7 63	*Clay*	*UC Moni form.*	*39.0638*	*0.0025*	*15.6812*	*0.0009*	*18.9258*	*0.0011*	*34°44′23.94″*	*33°13′51.24″*
C8 34	*Clay*	*UC Moni form.*	*38.8761*	*0.0010*	*15.6658*	*0.0004*	*18.8476*	*0.0004*	*34°44′35.52″*	*33°07′42.36″*
C8 35a	*Clay*	*UC Moni form.*	*38.9315*	*0.0011*	*15.6840*	*0.0004*	*18.8249*	*0.0005*	*34°44′15.24″*	*33°07′41.64″*
*C8 35a**	*Clay*	*UC Moni form.*	*38.9326*	*0.0010*	*15.6842*	*0.0004*	*18.8254*	*0.0004*	*34°44′15.24″*	*33°07′41.64″*
*C8 35a***	*Clay*	*UC Moni form.*	*38.9308*	*0.0010*	*15.6840*	*0.0004*	*18.8247*	*0.0004*	*34°44′15.24″*	*33°07′41.64″*
*C8 35a***	*Clay*	*UC Moni form.*	*38.9293*	*0.0011*	*15.6837*	*0.0004*	*18.8249*	*0.0005*	*34°44′15.24″*	*33°07′41.64″*
C8 35b	*Clay*	*UC Moni form.*	*38.9858*	*0.0009*	*15.6890*	*0.0003*	*18.8139*	*0.0004*	*34°44′15.24″*	*33°07′41.64″*
C9 34	Clay	UC Moni form.	38.9214	0.0028	15.6787	0.0012	18.8780	0.0012	/	/
C9 36	Clay	UC Moni form.	38.9713	0.0022	15.6871	0.0007	18.8116	0.0009	34°43′39.80″	33°10′04.50″
KKP 204	Clay	UC Kannaviou form.	38.8453	0.0028	15.6615	0.0010	18.8118	0.0011	/	/
C8 63a	*Umber*	*UC Perapedhi form.*	*38.7387*	*0.0011*	*15.6292*	*0.0004*	*18.7241*	*0.0005*	*34°48′0.42″*	*33°16′47.28″*
C8 63b	*Shale*	*UC Perapedhi form.*	*38.6792*	*0.0011*	*15.6160*	*0.0004*	*18.6610*	*0.0005*	*34°48′0.42″*	*33°16′47.28″*
C8 76a	*Umber*	*UC Perapedhi form.*	*38.6417*	*0.0011*	*15.6123*	*0.0004*	*18.6368*	*0.0005*	*34°46′32.46″*	*33°15′41.10″*
C8 76b	*Shale*	*UC Perapedhi form.*	*38.5202*	*0.0010*	*15.5918*	*0.0004*	*18.5157*	*0.0004*	*34°46′32.46″*	*33°15′41.10″*
KKP 202	Bentonitic clay	UC Perapedhi form.	38.8649	0.0023	15.6645	0.0009	18.8340	0.0010	/	/
KKP 202**	Bentonitic clay	UC Perapedhi form.	38.8616	0.0030	15.6641	0.0013	18.8332	0.0014	/	/
C7 O 2 Alt	*Clay*	*UC Volcanic seq.*	*38.9039*	*0.0043*	*15.6007*	*0.0012*	*18.8910*	*0.0014*	*34°55′38.46″*	*33°23′34.74″*
*C7 O 2 Alt**	*Clay*	*UC Volcanic seq.*	*38.9193*	*0.0031*	*15.6022*	*0.0012*	*18.9042*	*0.0014*	*34°55′38.46″*	*33°23′34.74″*
C7 O 2 Rock	*Rock*	*UC Volcanic seq.*	*38.9415*	*0.0052*	*15.6065*	*0.0021*	*18.8841*	*0.0023*	*34°55′38.46″*	*33°23′34.74″*
C7 O 12	*Clay*	*UC Volcanic seq.*	*38.8791*	*0.0018*	*15.6124*	*0.0007*	*18.8294*	*0.0008*	*34°55′47.94″*	*33°23′48.36″*
C8 11	Clay	UC Intrusive seq.	38.9618	0.0018	15.6401	0.0007	19.2742	0.0011	34°47′30.00″	33°13′56.40″
KKP201	Weather. gabbro	UC Plutonic seq.	38.9673	0.0016	15.6799	0.0005	18.9096	0.0006	/	/
KKP201**	Weather. gabbro	UC Plutonic seq.	38.9662	0.0021	15.6794	0.0008	18.9097	0.0010	/	/
C8 7	Weather. gabbro	UC Plutonic seq.	38.7954	0.0030	15.6013	0.0012	18.9580	0.0012	34°48′45.84″	33°11′56.16″
C8 8a	Weather. gabbro	UC Plutonic seq.	38.8224	0.0022	15.5780	0.0008	19.0510	0.0009	34°48′43.38″	33°11′54.24″
C8 8b	Weather. gabbro	UC Plutonic seq.	38.9820	0.0019	15.6735	0.0007	18.8984	0.0008	34°48′43.38″	33°11′54.24″
C8 9b	Weather. gabbro	UC Plutonic seq.	40.2163	0.0044	15.7128	0.0015	21.5311	0.0019	34°48′35.52″	33°11′44.64″
C8 70	Weather. gabbro	UC Plutonic seq.	38.7284	0.0024	15.5725	0.0007	18.8886	0.0010	34°48′44.70″	33°09′14.16″
C8 71	Weather. gabbro	UC Plutonic seq.	39.4792	0.0083	15.6901	0.0032	19.6286	0.0041	34°48′44.70″	33°09′14.16″
C8 71*	Weather. gabbro	UC Plutonic seq.	39.4858	0.0072	15.6892	0.0021	19.6233	0.0033	34°48′44.70″	33°09′14.16″
C9 49	Weather. gabbro	UC Plutonic seq.	38.4291	0.0019	15.6108	0.0010	18.5162	0.0008	34°48′45.80″	33°11′55.30″
C7 72a	Clay	UC Plutonic seq.	40.6408	0.0049	15.9574	0.0019	25.2754	0.0029	34°48′26.40″	33°11′20.64″
C8 69a	*Soil*		*38.9611*	*0.0012*	*15.6529*	*0.0004*	*18.8775*	*0.0005*	*34°51′16.14″*	*33°12′29.10″*
C9 40	Soil		38.6932	0.0020	15.5926	0.0008	18.8698	0.0009	34°47′49.00″	33°16′45.40″
C9 42	Soil		38.8036	0.0026	15.6278	0.0010	18.8457	0.0011	34°48′10.30″	33°16′46.40″
C9 44	Soil		38.9487	0.0027	15.6838	0.0012	18.8591	0.0011	34°48′58.40″	33°12′04.10″

* Duplicate.
** Replicate.

a

	C1	C2	C3	C4	C5	C1	C2	C3	C4	C5
V	**0.90**	-0.02	0.12	-0.07	0.25	**0.81**	0.00	0.01	0.00	0.06
Al	**0.87**	-0.12	-0.13	-0.01	-0.03	**0.76**	0.01	0.02	0.00	0.00
Fe	**0.84**	0.31	0.10	0.02	0.19	**0.71**	***0.10***	0.01	0.00	0.04
$^{206}Pb/^{204}Pb$	**0.76**	0.08	-0.26	0.00	-0.20	**0.58**	0.01	0.07	0.00	0.04
Na	**0.72**	-0.36	0.13	0.05	-0.12	**0.51**	***0.13***	0.02	0.00	0.02
$^{208}Pb/^{204}Pb$	***0.62***	-0.01	***-0.60***	0.02	-0.35	**0.39**	0.00	**0.36**	0.00	***0.12***
Mg	0.03	**0.95**	0.03	-0.03	-0.18	0.00	**0.90**	0.00	0.00	0.03
Ni	-0.17	**0.93**	-0.16	0.05	-0.07	0.03	**0.86**	0.03	0.00	0.00
Ca	0.06	**0.82**	0.36	0.01	-0.05	0.00	**0.68**	***0.13***	0.00	0.00
Ti	***0.53***	***-0.60***	0.18	0.20	0.26	***0.28***	**0.36**	0.03	0.04	0.07
$^{207}Pb/^{204}Pb$	0.08	-0.03	**-0.96**	0.01	-0.10	0.01	0.00	**0.92**	0.00	0.01
Mn	0.12	***0.49***	***0.62***	0.22	0.23	0.01	***0.24***	**0.38**	0.05	0.05
Sr	0.10	-0.21	***0.58***	0.29	0.41	0.01	0.04	**0.34**	0.09	***0.17***
Pb	0.04	0.05	-0.24	**0.80**	0.35	0.00	0.00	0.06	**0.64**	***0.12***
Si	0.33	0.27	0.19	**0.78**	-0.04	***0.11***	0.07	0.03	**0.61**	0.00
Rb	-0.14	-0.16	0.15	**0.76**	0.03	0.02	0.03	0.02	**0.58**	0.00
K	-0.30	***-0.50***	0.32	***0.54***	-0.17	0.09	***0.25***	***0.10***	**0.29**	0.03
Cu	0.10	-0.21	0.15	-0.06	**0.91**	0.01	0.04	0.02	0.00	**0.84**
Zn	-0.13	-0.03	0.30	0.34	**0.73**	0.02	0.00	0.09	***0.11***	**0.53**
					Eigv	4.35	3.72	2.64	2.43	2.13
					Var	22.9	19.6	13.9	12.8	11.2
					Acc	22.9	42.5	56.4	69.2	80.4

b

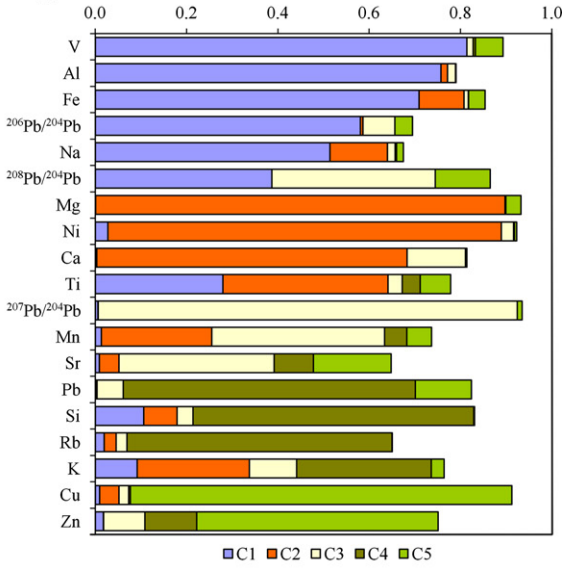

Fig. 3. (a) Factor loadings. In the PCA performed here, factor loadings represent correlation coefficients between the elements and the principal components; (b) communalities. The communality accounts for the proportion of each element's variance explained by the five extracted principal components. The total length of the bars is the communality of each element, while the sections represent the proportion of variance allocated in the principal components.

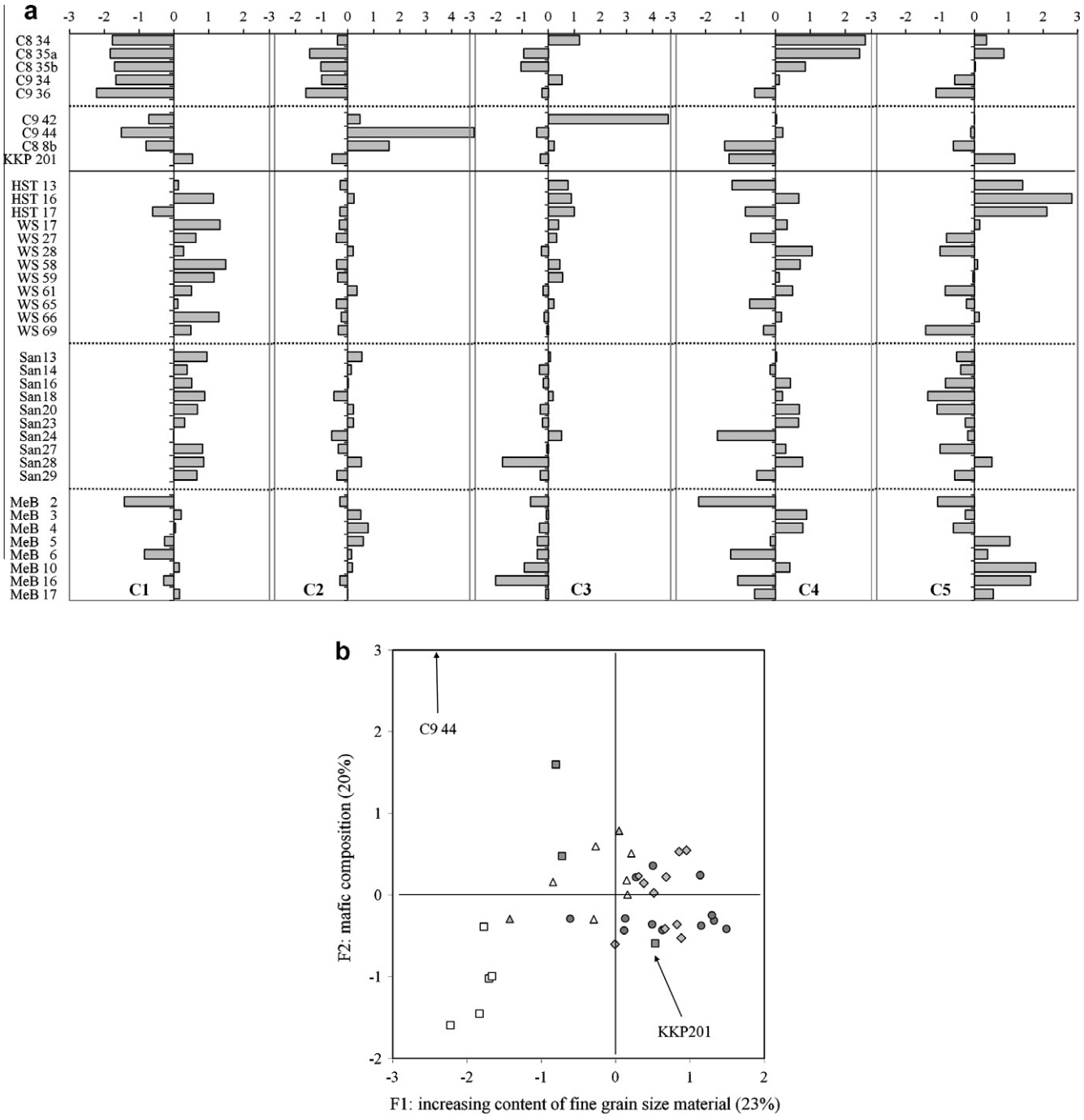

Fig. 4. (a) Factor scores of the five components in the different samples (pottery fragments and sediments); (b) C1–C2 projection showing the distribution of clays and sherds in the space defined by fine grain size content (C1) and mafic composition (C2). Open squares are Moni clays, light gray squares are weathered gabbros and soils, open triangles are White Slip II from Minet el-Beida, light gray diamonds are White Slip II from Sanidha and dark gray circles are White Slip II from Hala Sultan Tekke. Note that only clay KKP201 plots in the same compositional field of the sherds.

The third component, C3 (14% of variance), is associated almost exclusively with large negative loadings of $^{207}Pb/^{204}Pb$ (−0.96) (Fig. 3a and b). This component also accounts for part of the variance of Sr and Mn (Fig. 3b), but a detailed inspection shows that almost all the effect is related to clay sample C9 42 being a moderate outlier in this component. It is intriguing that the $^{207}Pb/^{204}Pb$ ratio is not correlated to the other isotopic ratios (at least that of the other uranogenic isotope, the $^{206}Pb/^{204}Pb$ ratio). However, from Fig. 4a it is clear that there is a difference between the ceramics: sherds from Hala Sultan Tekke have positive scores, sherds from Sanidha have close to zero scores, while sherds from Minet el-Beida have negative scores. In fact an ANOVA test indicates that sherds from Sanidha and Minet el-Beida have significantly higher $^{207}Pb/^{204}Pb$ ratios than samples from Hala Sultan Tekke. The only conclusion we can be advanced, at the moment, is that whatever the mineral phase (or phases) controlling the variations in $^{207}Pb/^{204}Pb$ ratios, it is not modeled by the chemical elements that have have analyzed.

The fourth component, C4 (13% of variance), is associated with large positive loadings of Rb, Pb and Si (0.76–0.80) and to a moderate positive loading of K (0.54) (Fig. 3a and b). This component accounts for most of the variation in Pb. Moni clays have high

positive C4 scores while the weathered gabbros have high negative scores (Fig. 4a). Within the pottery fragments, scores vary greatly. The elements of C4 indicate a felsic composition. Sediment samples with large positive scores in C2 contain amphibole, which is consistent with higher Ca, Mg and Ni concentrations; while illite/smectite-illite is more abundant in clays with higher C4 scores (samples of the Moni Formation). Thus, C2 suggests a more basic/ultrabasic and C4 a more acidic mineral component. Moni clays are enriched in elements associated with C4 but depleted in elements associated with C2. Clays from other soils and weathered gabbros are enriched in elements associated with C2. The evidence provided by C1, C2 and C4 chemical signatures, suggests that Moni clays were not used for the production of the White Slip II investigated here. This conclusion is consistent with the bulk mineralogy results.

Finally, C5 (11% of variance) is associated with large positive loadings of Cu and Zn (0.73–0.91) (Fig. 3a and b). Most of the sherds from Minet el-Beida and a few from Hala Sultan Tekke have high positive scores in C5, which indicates higher Cu and Zn contents in these samples (Fig. 4a). In the geological context of the Troodos Ophiolite foothills of Sanidha area, these Cu and Zn contents can be related to sulfide deposits. It is worth noting that Pb occurs in these sulfide ores (Gale and Stos-Gale, 1982).

PCA results also seem to indicate that the $^{206}Pb/^{204}Pb$ and $^{208}Pb/^{204}Pb$ ratios vary with C1 (Fig. 5). The higher the fine fraction content, the higher these two isotope ratios. This means that the grain-size selection performed on the clays prior to pottery production influenced the isotopic composition, but in a limited range that does not affect the possibility of linking the pottery to its original raw material (Fig. 2c). This process does not affect the $^{207}Pb/^{204}Pb$ ratio (Fig. 5).

The fifth component, C5 (related to Cu and Zn content), controls part of the Pb content variability (Pb_{res} in Fig. 6a). As the Cu and Zn contents increase, the Pb_{res} content also increases but not in the same proportion in all the pottery groups. Sanidha sherds and Hala Sultan Tekke sherds share a similar trend. The Minet el-Beida samples are divided in two groups according to this component. Two of the three samples (White Slip II) having an isotopic composition similar to that of Sanidha White Slip II show a link between Pb_{res} and Cu-Zn contents that is similar to White Slip II from Sanidha. Six samples from Minet el-Beida (2 White Slip II and 3 White Slip II late which do not share the isotopic composition of Sanidha White Slip II and one White Slip II that does share it), show a stronger influence on Pb_{res}; because the Pb_{res} content is more affected by the Cu–Zn content than in the other pottery groups (the slope of the regression is twice for these samples than for the other group, Fig. 6a). The fifth component, related to the presence of Cu–Zn–(Pb) bearing sulfides, also controls part of the isotopic variability (Fig. 6b). Sulfides seem to increase total Pb concentration at the same time they produce a decrease in the isotopic ratios (Fig. 6a and b).

The White Slip II from Sanidha, most White Slip II from Hala Sultan Tekke, and three White Slip II from Minet el-Beida, share a common origin that corresponds to the local weathered gabbros outcropping in the proximity of Sanidha. This conclusion is in agreement with that of Gomez et al. (1995). Clearly, these samples were processed by removing part of the coarse fraction prior to pottery making.

The lower values of isotopic ratios of some White Slip II sherds from Hala Sultan Tekke could be related to a higher content of sulfides in the clay matrix. Indeed, Booij et al. (2000) showed that sulfides have lower Pb isotope ratios than their source rocks, in this case greenschist samples from the Troodos Ophiolite. The lower isotopic values of some of the pottery samples analyzed in the present study can be interpreted as the result of the presence of sulfides in the clay derived from the greenschist facies gabbros that

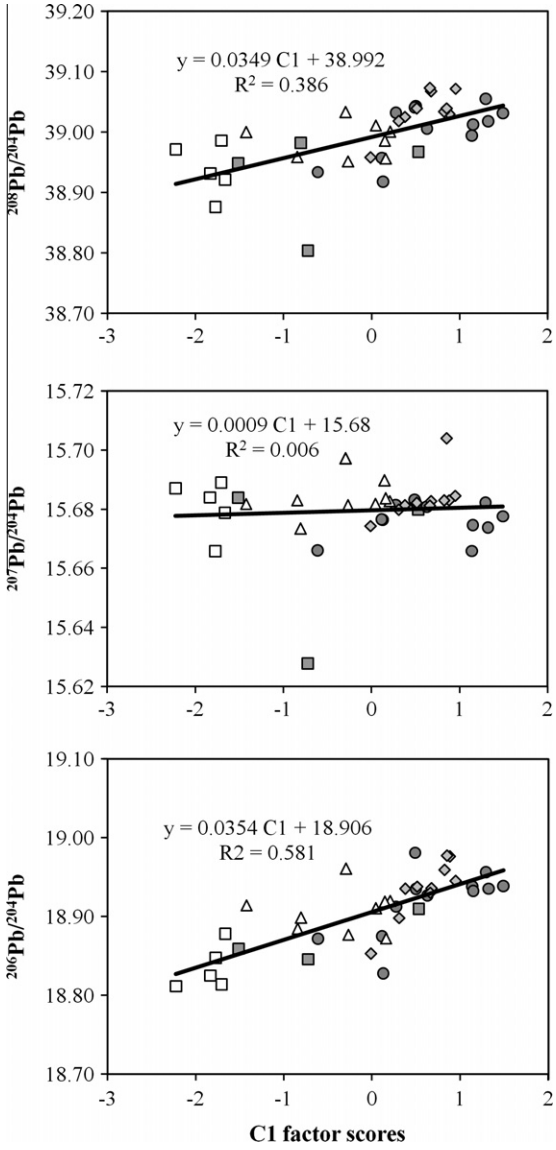

Fig. 5. Scattergram showing the isotopic composition vs the factor scores of C1 in clays and pottery fragments. Higher positive scores indicate enrichment in finer grains and thus a higher grain-size selection. Symbols as in Fig. 4.

were used for White Slip II production. In this context, in terms of sources, the variability in isotopic composition of some White Slip II sherds from Hala Sultan Tekke could be explained by a variability of the sulfide content of the clays used for their production. Nevertheless, these White Slip II sherds from Hala Sultan Tekke and Sanidha most likely originated from the same source and were produced using very similar raw materials.

The last three samples from Hala Sultan Tekke, which have an isolated isotopic composition (WS 33, WS 35 and WS 36), were not included in the PCA. Their very different signature could be explained by seawater contamination of the clay used for their production. Such a contamination is likely because they show an Eu anomaly (Hatcher, personal communication) compatible with seawater contamination. On-going studies using Sr isotopes could confirm or refute this hypothesis.

In her investigation of ceramics from Sanidha, Herscher (in Todd and Hadjicosti (1991)) indicated that the dominant style of White Slip II was similar to that of ceramics excavated in Kalavasos-*Ayios Dhimitrios* and to that from the sherd deposit from Hala Sultan Tekke investigated by Öbrink (1979). Most of the White Slip

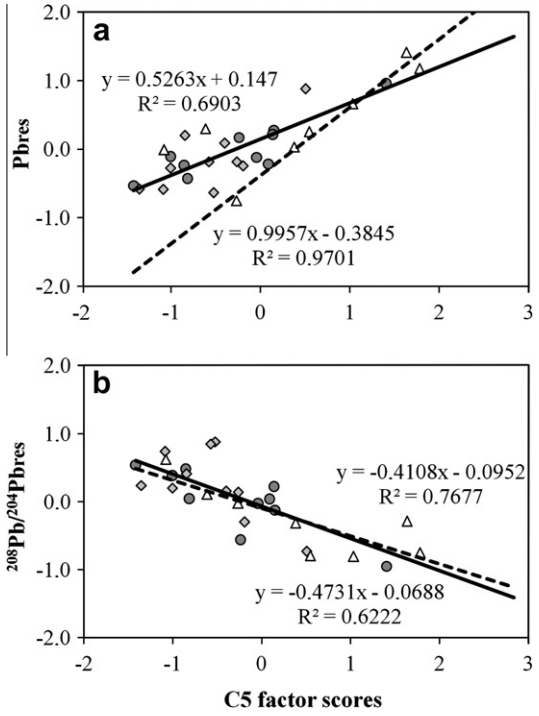

Fig. 6. (a) Relationship between part of the total Pb content (Pbres) and C5 factor scores (indicative of a Cu–Zn sulfide bearing phase); (b) relationship between part of the isotopic composition ($^{206}Pb/^{204}Pb$res) and C5 factor scores. Symbols as in Figs. 4 and 5, except for the light gray triangles showing White Slip II sherds from Minet el-Beida that have a similar isotopic composition to White Slip II sherds from Sanidha. Pbres: since the regression of C4 scores vs Pb accounts for Pb in felsic minerals (64% of Pb variance), the residual term is calculated by detrending total Pb concentration from C4: obtaining for every sample the difference between the observed (concentration in the sample) and expected (estimated based on the linear equation of the regression function) values. Residuals (Pbres) are assumed to represent the fraction of Pb related to non-felsic sources. $^{206}Pb/^{204}Pb$res: in a similar way, the residual isotopic signal is obtained in two steps (since it has two major controls, C1 and C3): first it is detrended from C1, and then the obtained residuals are detrended from the effect of C3. The high correlation of Pbres and $^{206}Pb/^{204}Pb$res with C5 scores point to a residual dominant effect of a sulfide phase.

II from Hala Sultan Tekke analyzed here are part of this assemblage studied by Öbrink. The results also favor the use of a common clay source for the pottery made at Sanidha and for the White Slip II sherds assemblage from Hala Sultan Tekke studied here. However, because no clear source can be proposed for samples WS 33, WS 35 and WS 36, this conclusion is not valid for these three sherds, so far.

The sherds from Minet el-Beida (2 White Slip II and 3 White Slip II late), which do not share the isotopic composition of Sanidha, show a different relationship between Pb and Cu-Zn contents. Moreover, the clay used for their production was processed in a significantly different way. It is less enriched in fine grain size fraction than the Sanidha pottery (close to zero or negative C1 scores; Fig. 6b). This clearly suggests that this White Slip II group originates from another source with a different mode of preparation of the clay. The White Slip sherds excavated in Tomb III in Minet el-Beida originate from two different sources, one of them being consistent with a Sanidha origin and another with a, so far, unknown clay that could come from a different location in the foothills of the Troodos Ophiolite or perhaps from Syria.

7. Conclusions

The Pb isotopic composition of the pottery production in Sanidha is homogeneous and confirms the effectiveness of the method to identify pottery assemblages. Lead isotopic analysis also constitutes an efficient tool to further refine the links between the pottery sherds to the local clays derived from the weathering of the surrounding lithologies (in this case the gabbros). Here, the good concordance of the Pb isotope results with the study of Gomez et al. (1995) reinforces the identification of the weathered gabbro as the source for pottery production in Sanidha. However, the former hypothesis (Renson et al., 2011) that proposed clays from the Moni formation as a possible raw material for White Slip II ware production can definitively be discarded. The isotopic signature of the White Slip II ware pottery set from Hala Sultan Tekke corresponds well with a Sanidha source. Most likely the Sanidha and Hala Sultan Tekke material studied here share a similar origin, derived from the weathered gabbro, outcropping in the vicinity of Sanidha.

Two different origins can be proposed for White Slip II ware from Minet el-Beida. Some of the sherds share a common origin with White Slip II ware from Sanidha, and were most likely produced at Sanidha. Another group of sherd samples is most likely derived from another source, not yet identified. It should be searched for in the foothills of the Troodos Ophiolite or perhaps in the vicinity of Minet el-Beida.

This study also provides evidence for a grain-size selection and thus of a well defined and specific preparation of the clays prior to the White Slip II ware production. However, this grain size sorting and the selection of the finer fraction occurred without any major modification of the Pb isotopic composition.

The approach proposed here that includes Pb isotope analysis is indisputably efficient for identifying different groups within White Slip ware pottery, to link White Slip ware pottery to their clay sources and also to identify processes applied to clays prior to pottery making. The use of such an approach on further White Slip fragments and clays from the surroundings of the Troodos should allow a better understanding of this pottery ware production and distribution, which would improve knowledge on links and exchange between Cyprus and numerous regions in the Eastern Mediterranean. This type of approach is also encouraged at other similar archeological sites containing a variety of ceramics and different clay raw materials in the vicinity. This study confirms the utility of using Pb isotopic characterization for pottery provenance as well as the effectiveness and diagnostic significance of Pb isotopic analysis within multiproxy approaches.

Acknowledgements

This study is supported by the Research Foundation Flanders (FWO Grants KN137 to Karin Nys and G.0585.06 to Philippe Claeys and Frank Vanhaecke) and the Research Council of the Vrije Universiteit Brussel (Grant HOA11 to Karin Nys and Philippe Claeys). The WD-XRF acquisition, set-up and optimisation, was made possible through a research grant from the Kempe Foundation to Richard Bindler, which also provided a post doc fellowship to F.D.V. Additional support was provided by the Swedish Research Council (grant to Richard Bindler). We warmly thank the Musée d'Archéologie Nationale de Saint-Germain-en-Laye for allowing the sampling of material from Ugarit and for providing room in the laboratory during the sampling. We are grateful to Alison South and Ian Todd for providing pottery samples from Sanidha and to the late Professor Paul Åström for the White Slip sherds from Hala Sultan Tekke. Thank you to Claude Maerschalk, Jeroen De Jonge and Vinciane Debaille from Université Libre de Bruxelles and Kris Latruwe from University of Gent for their help during the laboratory work and the measurements at the MC-ICP-MS, to Nathalie Fagel (University of Liège) for spending time on some XRD spectra interpretation, to Oscar Steenhaut (Vrije Universiteit Brussel) for his assistance during the measurements on the SEM-EDX and to

Céline Martin (Vrije Universiteit Brussel) for helping with the SEM-EDX data treatment.

References

Adan-Bayewitz, D., Perlman, I., 1985. Local pottery provenience studies: a role for clay analysis. Archaeometry 27, 203–217.

Artzy, M., Perlman, I., Asaro, F., 1981. Cypriote pottery at Ras Shamra. Isr. Explor. J. 31, 37–47.

Asaro, F., Adan-Bayewitz, D., 2007. The history of the Lawrence Berkeley National Laboratory instrumental neutron activation analysis programme for archaeological and geological materials. Archaeometry 49, 201–214.

Åström, P., 1986. Hala Sultan Tekke – an international harbour town of the Late Cypriot Bronze Age. Opusc. Athen. XVI, 7–17.

Åström, P., Nys, K., 2007. Tomb 24. In: Åström, P., Nys, K. (Eds.), Hala Sultan Tekke 12. Tomb 24, Stone Anchors, Faunal Remains and Pottery Provenance. Studies in Mediterranaean Archaeology, 45(12), Paul Åströms Förlag, Sävedalen, pp. 6–30.

Baxter, M.J., 1995. Standardization and transformation in principal component analysis, with applications to archaeometry. Appl. Statist. 44, 513–527.

Baxter, M.J., 1999. Detecting multivariate outliers in artifact compositional data. Archaeometry 41, 321–338.

Baxter, M.J., 2001. Statistical modelling of artifact compositional data. Archaeometry 43, 131–147.

Beckman, G., 1996. Hittite Diplomatic Texts, SBL Writings from the Ancient World, vol. 7, Atlanta, Georgia.

Ben-Shlomo, D., Maier, A.M., Mommsen, H., 2007. Neutron activation and petrographic analysis of selected Late Bronze Age and Iron Age pottery from Tell es-Safi/Gath, Israel. J. Archaeol. Sci. 35, 956–964.

Booij, E., Bettison-Varga, L., Farthing, D., Staudigel, H., 2000. Pb-isotope systematics of a fossil hydrothermal system from the Troodos ophiolite, Cyprus: evidence for a polyphased alteration history. Geochim. Cosmochim. Acta 64, 3559–3569.

Cook, H.E., Johnson, P.D., Matti, J.C., Zemmels, I., 1975. Methods of sample preparation and X-ray diffraction data analysis, X-ray Mineralogy Laboratory. In: Kaneps, A.G. (Ed.), Initial Reports of the DSDP. Print Office, Washington, DC, pp. 997–1007.

Courtois, L., Velde, B., 1980. Petrographic and Electron Microprobe studies of Cypriote White Slip Ware (Late Bronze Age). Revue d'Archéométrie, Actes du XX Symposium International d'Archéométrie, vol. III (Bulletin de liaison du Groupe des Méthodes Physiques et Chimiques de l'Archéologie), Supplément, pp. 37–43.

Courtois, L., Velde, B., 1989. Petrographic studies of pottery (preliminary results). In: South, A.K. (Ed.), Kalavasos-Ayios Dhimitrios II. Ceramics, Objects, Tombs, Specialist Studies. Vasilikos Valley Project 3. Studies in Mediterranaean Archaeology 71(3). Paul Åströms Förlag, Göteborg, pp. 73–77.

De Vleeschouwer, F., Renson, V., Claeys, P., Nys, K., Bindler, R., 2011. Quantitative WD-XRF calibration for small ceramic samples and their source material. Geoarchaeology 26, 440–450.

Eriksson, K.O., 2007. The Creative Independence of Late Bronze Age Cyprus. An Account of the Archaeological Importance of White Slip Ware, Verlag der Österreichischen Akademie der Wissenschaften, Denkschriften der Gesamtakademie, Band XXXVIII, Wien.

Eriksson, L., Johansson, E., Kettaneh-Wold, N., Wold, S., 1999. Introduction to Multi- and Mega-Variate Data Analysis using Projection Methods (PCA & PLS). Umetrics AB, Umea.

Freestone, I.C., Meeks, N.D., Middleton, A.P., 1985. Retention of phosphate in buried ceramics: an electron microbeam approach. Archaeometry 27, 161–177.

Gale, N.H., Stos-Gale, Z.A., 1982. Bronze Age copper sources in the Mediterranean: a new approach. Science 216, 11–18.

Galer, S.J.G., Abouchami, W., 1998. Practical applications of lead triple spiking correction of instrumental mass discrimination. Mineral. Mag. 62A, 491–492.

Gass, I.G., MacLeod, C.J., Murton, B.J., Panayiotou, A., Simonian, K.O., Xenophontos, C., 1994. The Geology of the Southern Troodos Transform Fault Zone. Geological Survey Department, Nicosia.

Gomez, B., Doherty, C., 2000. A preliminary petrographic analysis of Cypriot White Slip II ware. Archaeometry 42, 109–118.

Gomez, B., Rautman, M.L., Neff, H., Glascock, M.D., 1995. Clays related to the production of White Slip Ware. Rep. Dep. Antiq. Cyprus, pp. 113–118.

Gomez, B., Neff, H., Rautman, M.L., Vaughan, S.J., Glascock, M.D., 2002. The source provenance of Bronze Age and Roman pottery from Cyprus. Archaeometry 44, 23–36.

GSD, 1995. Geological Survey Department of Cyprus, 1995, Geological Map of Cyprus, 1:250000.

Hamelin, B., Dupré, B., Allègre, C.J., 1984. The lead isotope systematics of ophiolite complexes. Earth Planet. Sci. Lett. 67, 351–366.

Hamelin, B., Dupré, B., Brévart, O., Allègre, C.J., 1988. Metallogenesis at paleo-spreading centers: lead isotopes in sulfides, rocks and sediments from the Troodos Ophiolite (Cyprus). Chem. Geol. 68, 229–238.

Harlavan, Y., Erel, Y., Blum, J.D., 1998. Systematic changes in lead isotopic composition with soil age in glacial granitic terrains. Geochim. Cosmochim. Acta 62, 33–46.

Kennett, D.J., Anderson, A.J., Cruz, M.J., Clark, G.R., Summerhayes, G.R., 2004. Geochemical characterization of Lapita pottery via Inductively Coupled Plasma-Mass Spectrometry (ICP-MS). Archaeometry 46, 35–46.

Knapp, A.B., Cherry, J.F. (Eds.), 1994. Provenience Studies and Bronze Age Cyprus, Production, Exchange and Politico-Economic Change. Monographs in World Archaeology, vol. 21. Prehistory Press, Madison, Wisconsin.

Lackenbacher, S., 2002. Textes Akkadiens d'Ugarit, LAPO 20. Éditions du Cerf, Paris.

Marchegay, S., 1999. Les tombes d'Ougarit : architecture, localisation et relation avec l'habitat. Unpublished PhD. Univ. Lumière Lyon-2.

Mommsen, H., 2003. Attic pottery production, imports, and exports during the Mycenaean period by Neutron Activation Analysis. Mediter. Archaeol. Archaeom. 3, 13–30.

Moore, D.M., Reynolds, R.C., 1989. X-Ray Diffraction and the Identification and Analysis of Clay Minerals. Oxford University Press.

Moran, W.L., 1992. The Amarna Letters. Johns Hopkins University Press, Baltimore and London.

Nobre-Silva, I.G., Weis, D., Barling, J., Scoates, J.S., 2009. Leaching systematics and matrix elimination for the determination of ocean island basalts. Geochem. Geophys. Geosyst. 10 (8), Q08012. http://dx.doi.org/10.1029/2009GC002537.

Öbrink, U., 1979. A sherd deposit in Area 22, Hala Sultan Tekke 6, Studies in Mediterranaean Archaeology 45 (6), Göteborg.

Popham, M.R., 1972. White slip ware. In: Aström, P. (Ed.), The Swedish Cyprus Expedition IV: 1C. Swedish Cyprus Expedition, Lund, pp. 431–471.

Rautman, M.L., Gomez, B., Neff, H., Glascock, M.D., 1993. Neutron activation analysis of Late Roman ceramics from Kalavasos-Kopetra and the environs of the Vasilikos valley. Rep. Dep. Antiq. Cyprus, pp. 233–264.

Renson, V., Coenaerts, J., Nys, K., Mattielli, N., Åström, P., Claeys, Ph., 2007. Provenance determination of pottery from Hala Sultan Tekke using lead isotopic analysis: preliminary results. In: Åström, P., Nys, K. (Eds.), Hala Sultan Tekke 12. Tomb 24, Stone Anchors, Faunal Remains and Pottery Provenance. Studies in Mediterranaean Archaeology 45(12). Paul Åströms Förlag, Sävedalen, pp. 53–62.

Renson, V., Coenaerts, J., Nys, K., Mattielli, N., Vanhaecke, F., Fagel, N., Claeys, Ph., 2011. Lead isotopic analysis for the identification of Late Bronze Age pottery from Hala Sultan Tekke (Cyprus). Archaeometry 53, 37–57.

Schaeffer, C.F.A., 1929. Les fouilles de Minet-El-Beida et de Ras Shamra (campagnes du printemps 1929). Syria X, 285–297.

Schaeffer, C.F.A., 1949. Ugaritica II. Librairie orientaliste Paul Geuthner, Paris.

Spooner, E.T.C., Gale, N.H., 1982. Pb isotopic composition of ophiolitic volcanogenic sulphide deposits, Troodos Complex, Cyprus. Nature 296, 239–242.

Todd, I.A., 1990. Sanidha-*Moutti tou Ayiou Serkou*: a Late Bronze Age Site in the Troodos Foothills. Archaeol. Cypria 2, 53–62.

Todd, I.A., 2000. Excavations at Sanidha. A Late Bronze Age ceramic manufacturing centre. In: Ioannides, G.C., Hadjistyllis, S. (Eds.), 3rd Internat. Congress of Cypriote Studies. Lefkosia, 16–20 April 1996, Lefkosia 1, pp. 301–324.

Todd, I.A., 2004. The Field Survey of the Vasilikos Valley 1. Vasilikos Valley Project 9, Studies in Mediterranean Archaeology LXXI: 9. Paul Åströms Förlag, Sävedalen.

Todd, I.A., Hadjicosti, M., 1991. Excavations at Sanida 1990. Rep. Dep. Antiq. Cyprus, pp. 37–74.

Tschegg, C., Hein, I., Ntaflos, T., 2008. State of the art multi-analytical geoscientific approach to identify Cypriot Bichrome Wheelmade Ware reproduction in the Eastern Nile delta (Egypt). J. Archaeol. Sci. 35, 1134–1147.

Tschegg, C., Ntaflos, T., Hein, I., 2009. Integrated geological, petrologic and geochemical approach to establish source material and technology of Late Cypriot Bronze Age Plain White ware ceramics. J. Archaeol. Sci. 36, 1103–1114.

Weis, D., Kieffer, B., Maerschalk, C., Barling, J., de Jong, J., Williams, G.A., Hanano, D., Pretorius, W., Mattielli, N., Scoates, J.S., Goolaerts, G., Friedman, R.M., Mahoney, J.B., 2006. High-precision isotopic characterization of USGS reference materials by TIMS and MC-ICP-MS. Geochem. Geophys. Geosyst. 7 (8), Q08006. http://dx.doi.org/10.1029/2006GC001283.

White, W.M., Albarède, F., Télouk, P., 2000. High-precision isotopic characterization of USGS reference materials by TIMS and MC-ICP. High-precision analysis of Pb isotope ratios by multi-collector ICP-MS. Chem. Geol. 167, 257–270.

Yon, M., 1981. Dictionnaire illustré multilingue de la céramique du Proche Orient ancient, Collection de la Maison de l'Orient Méditérranéen 10, Série archéologique 7. Lyon.

Yon, M., Karageorghis, V., Hirschfeld, N., 2000. Céramiques Mycéniennes d'Ougarit, RSO XIII, Fondation A.G. Leventis – ERC, Nicosia.